PHYSICS for ECONOMY

Vol. 1, No. 1, 2017

Issued with the consent of the Rector

Editor in Chief
Publishing House of Rzeszow University of Technology
Grzegorz OSTASZ

Composition of the Scientific Papers Council
of the Faculty of Mathematics and Applied Physics
of Rzeszow University of Technology
„Physics for Economy"
Tomasz WIĘCEK – chairman (Poland)
Dorota JAKUBCZYK – editorial assistant (Poland)

Editor in Chief
Tomasz WIĘCEK (Poland)

Editorial Committee (Thematic editors)
Henryka CZYŻ (Poland), Vitalii DUGAEV (Poland)
Czesław JASIUKIEWICZ (Poland)

Statistical editor
Andrzej WASILEWSKI (Poland)

Members of editorial staff
Michał INGLOT (Poland), Ryszard STAGRACZYŃSKI (Poland)
Gaweł ŻYŁA (Poland)

Project of the cover
Bożena ŚWIDER

The printed version of the Journal is an original version.

Publisher: Publishing House of Rzeszow University of Technology
Powstańców Warszawy 12, 35-959 Rzeszow (e-mail: oficyna@prz.edu.pl)
http://oficyna.prz.edu.pl

Editorial Office: Rzeszow University of Technology, The Faculty of Mathematics and Applied Physics,
Powstańców Warszawy 8, 35-959 Rzeszów (e-mail: phyeco@prz.edu.pl)
Additional information and an imprint – p. 65

SPIS TREŚCI

Henryka CZYŻ, Tadeusz JASIŃSKI: Physics in medicine and economy of contemporary society 5

Paulina KALAMARZ, Magdalena ZAGROBELNA, Leszek PYZIAK: Focusing ultrasounds beam 15

Marzena MALICKA, Mateusz MALICKI: Measurement of the intensity of the electric field of the radio wave emitted by selected mobile phones 27

Jan A. MAMCZUR: A proof of non-existence of self-imaging phenomenon in incoherent case 35

Aleksander SOKOŁOWSKI, Tomasz. WIĘCEK: A new algorithm for testing the properties of nonwoven fabrics 41

Feliks STACHOWICZ, Marta WÓJCIK: Ecological and economical benefits from sewage sludge hygienisation with the use of lime in a medium-size treatment plant 49

Henryka CZYŻ[1]
Tadeusz JASIŃSKI[2]

PHYSICS IN MEDICINE AND ECONOMY OF CONTEMPORARY SOCIETY

This paper describes the main methods of separating blood into components. The most common methods used in medicinal practice include centrifugation and filtration. Currently, there has been a lot of research on the application of ultrasound as the new, innovative method of separation of blood components. Ultrasound use is a theoretically elaborated method and experimental research is in process with the aim of its implementation in medical diagnostics. Contemporary societies are aware of the importance of findings of physics as well as of the fact that our everyday life is strongly connected to physics and to technical devices that have been created on the basis of its fundamental laws.

Keywords: laws of physics, human blood, centrifugation, filtration, acoustic standing wave, medical applications of ultrasound

INTRODUCTION

Physics is a cornerstone of contemporary economy, civilization and culture. It makes it possible to learn about environment and discover natural laws from the smallest particles to the entire universe. Technical sciences make use of findings of physicists and present application possibilities of physics in various sectors of commerce, economy and medicine. Laws and terms of physics are also used to explain biological processes. In the 21st century physics has become a driving force for the scientific, technological and economic development of the entire world.

Diagnostic medicine is based on physical sciences due to which it is possible, inter alia, to precisely specify the composition of human blood. Blood structure allows for a separation of red cells from plasma. Since blood cells perform a variety of biological functions and take part in many disease processes, they are widely researched and, therefore, it is essential from the point of view of diagnostics to define blood composition [1]. Recently, researchers from all over the coun-

[1] Corresponding author: Heryka Czyż, Rzeszow University of Technology, Powstancow Warszawy 8, 35-959 Rzeszow, Poland, phone: (17) 8651908, e-mail: hczyz@prz.edu.pl
[2] Tadeusz Jasiński, Rzeszow University of Technology, e-mail: jasinski@prz.edu.pl

try have been involved in developing cooperation with economic environments which are equally interested in working with scientific entities. Physics' contribution is, furthermore, of great importance for solving economic, civilizational and medical problems.

This paper presents an analysis of physical processes underlying traditional methods of blood separation as well as it outlines an innovative method that makes use of ultrasound [2].

The conventional methods for separating blood components include centrifugation and filtration. These methods are a cornerstone of contemporary diagnostic medicine being subject to constant improvements. New, innovative and efficient methods are also sought. One of them is blood separation using ultrasound with parameters selected appropriately to the physical parameters of blood components [3, 4].

This topic is now subject of an extensive research both theoretical and experimental.

1. HUMAN BLOOD – COMPOSITION, PROPERTIES, CHARACTERISTICS

Since blood constantly flows through the human organs, it is an important source of information on the body condition and a fundamental diagnostic specimen which can be easily and safely taken from the patient. It is after losing 30% of the total blood volume that blood loss is dangerous and life-threatening [5].

Blood is a suspension of erythrocytes, platelets and leukocytes in blood plasma. Plasma is composed of water (approx. 90%), organic materials (mainly proteins), organic compounds (such as glucose) and inorganic materials (mainly chlorine and sodium ions). The ratio of the volume of erythrocytes to the total volume of blood is called hematocrit (HCT). Hematocrit value is expressed as a percentage. The normal hematocrit for adult women ranges from 37 to 47% whereas for adult men from 42 to 54% [5].

Marure erythrocytes have round, biconcave shape and an average diameter of 7 to 7.5 micrometers [5]. They have high elasticity due to which they become deformed while flowing through narrow capillaries.

Blood and its components play many important roles in the human body and all life processes.

Human blood is known as a liquid connective tissue and it performs many important functions such as coagulation, transportation and thermoregulation. Transportation is mostly related to oxygen transport to the cells and removal of carbon dioxide from organs. In addition, blood removes metabolic waste products such as uric acid. High water content in blood helps to ensure thermal regulation of the body.

The principal function of red cells is bonding of oxygen and its transport to tissues as well as transport of carbon dioxide from tissues to the respiratory organs. Erythrocytes are produced by bone marrow that generates about 200 billion of new red blood cells every day with maximal lifespan of 120 days [5].

An important parameter of every liquid is viscosity defined as a fluid's internal resistance to flow. Viscosity η is the ratio of shear stress τ and shear rate γ [6]:

$$\eta = \frac{\tau}{\gamma} \tag{1}$$

The SI unit for viscosity is the Pascal-second $1\ \mathrm{Pa \cdot s} = \frac{1\ \mathrm{kg}}{1\ \mathrm{m \cdot s}}$. Shear stress τ (applied parallel to the material) is defined as the ratio of the force causing displacement of layer to the material surface over which the force is applied:

$$\gamma = \frac{T_F}{S} \tag{2}$$

Shear rate is the ratio of layer displacement velocity and distance between layers: $\tau = \frac{v}{x}$.

According to Newton's Law, the friction force between two layers of a fluid is directly proportional to the difference in velocity of the displacing layers Δu and inversely proportional to the distance between the layers Δx; and it also depends on the viscosity of a fluid η.

$$F_T = \eta S_P \frac{\Delta u}{\Delta x} \tag{3}$$

where: S_P – plate surface. Whole blood is a non-Newtonian fluid i.e. its viscosity is not constant (it depends on the shear rate γ), hence it does not follow the Newton's Law.

The Table 1 presents the viscosity of some physiological fluids [6].

Viscosity of water in the temperature of 20°C is $\eta_0 = 1.0 \cdot 10^{-3} \frac{\mathrm{Ns}}{\mathrm{m}^2}$. Some of the important factors affecting viscosity of blood include:

- shear rate – viscosity increases with the decrease of shear rate;
- temperature – with the rise of temperature viscosity decreases;
- HCT – the lower hematocrit, the lower viscosity.

Blood is a heterogeneous mixture.

Table 1. The viscosity of some physiological fluids [6]

Fluid	$\frac{\eta}{\eta_0}$ on average	η, $\frac{\mathrm{Ns}}{\mathrm{m}^2}$
Whole blood	4.75	$4.75 \cdot 10^{-3}$
Plasma	2.01	$2.01 \cdot 10^{-3}$
Serum	1.88	$1.88 \cdot 10^{-3}$

2. FALLING OF BLOOD CELLS IN THE GRAVITATIONAL FIELD

Spontaneous fall of the blood cells is known as sedimentation. The process of sedimentation is a result of gravitational force and begins just after taking blood sample from a patient. Because of their heaviness erythrocytes fall to the bottom of the tube creating dark purple suspension which is approximately 45% of the total volume [5]. Above the layer of red cells, a creamy buffy coat is created by leucocytes and platelets.

The next layer is made by plasma which is a straw coloured liquid component constituting not more than 55% of the tube volume. It is after more than ten hours that sedimentation ceases.

In order to accelerate this process, laboratory centrifuges are used for separation of blood into components by spinning a sample with an anti-coagulant (compound preventing from clotting and enabling centrifugation of serum). Measuring the erythrocyte sedimentation rate (ESR) is known as Biernacki's Reaction (OB) and it is one of the most common tests taken.

The value of ESR depends on many factors ranging from 7 to 15 mm/h for adult women and from 5 to 10 mm/h for men [5]. The test should be performed at a constant temperature (around 20°C) without exposure to any external stimuli. Sedimentation rate while spinning depends on the protein content as well as the shape, size and quantity of red blood cells.

3. CONVENTIONAL METHODS FOR SEPARATING BLOOD INTO COMPONENTS

3.1. Centrifugation

Centrifugation is one of the traditional methods for separation of blood into components and it is based on the application of the centrifugal force [1]. The process uses differences in density of cells subject to test. A centrifuge is equipped with a rotor that regulates the velocity of spinning. Since the temperature affects separation of blood components significantly, thermoregulation systems are applied to keep temperature constant.

An important part of a centrifuge is a vacuum chamber in which a rotor is installed. The vacuum eliminates friction that heats the rotor when in contact with

air. Centrifugation requires samples to be put in hermetically sealed containers. While spinning, centrifugal force that is hundreds of thousands times bigger than gravity is created in rotor.

Thanks to centrifugation it is possible to shorten the time of blood fractionation. Specific parameters must be set to carry out the whole process properly. During validation of the process parameters must be modified in a way that ensures compliance of blood components with quality control standards.

Some types of centrifuges are equipped with additional functions such as acceleration of rotating or stop function [1].

3.2. Filtering

Membrane is a continuous phase which forms an obstacle for the components of a solution [7]. Particles which flow through the membrane at different velocity are retained by permeate. The process takes place in membrane module to ensure the flow of separated fluid in parallel or perpendicular direction to the membrane surface. For the purposes of dialysis crossflow filtration is used in which the feed solution flows parallel to the membrane surface while the direction of solution flow and permeate is perpendicular. Apart from permeate, retentate is obtained (feed solution without components that went to the permeate).

In dialyses porous membranes are used (Fig. 1) in which the separation is based on sieve effect and the factor determining effective separation is the size of pores. Transportation through membrane is due to the application of a proper driving force which for membrane processes is usually the difference in concentration, pressure, electric potential or temperature.

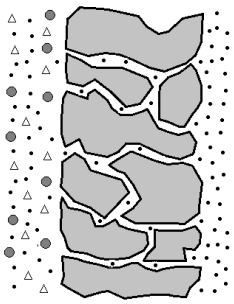

Fig. 1. Structure of porous membrane.
Own elaboration based on [7]

Membrane performance is characterized by two parameters:

- permeate stream describing membrane efficiency;
- efficiency characterizing membrane filtration capacity.

Permeate stream J_i is one of the following parameters: weight, volume or number of moles of a substance P_i, which passes through unit surface area of a membrane S_m per unit time [7]:

$$J_i = \frac{P_i}{S_m t_p} \tag{4}$$

expressed in the following unit, $\frac{\text{kg}}{\text{m}^2 \cdot \text{s}}$.

Membrane effeciency is defined by the following parameters: selectivity β or rejection coefficient R_r. Selectivity β is defined as the ratio of permeability of components of a fluid through the membrane and it is expressed by the following equation [7]:

$$\beta_{\frac{A}{B}} = \frac{y_A}{y_B} \cdot \frac{x_B}{x_A} \tag{5}$$

where: y_A, y_B – concentration of component A, B in permeate; x_A, x_B – concentration of component A, B in feed solution.

Rejection coefficient R_r is defined by the following equation [7]:

$$R_r = \frac{C_n - C_p}{C_n} = 1 - \frac{C_p}{C_n} \tag{6}$$

where: C_n – concentration of a given component in feed solution; C_p – concentration of a given component in permeate.

Membranes are used for adhesive and adsorbent filters to separate leucocytes and erythrocytes from the whole blood. Membrane with a proper diameter of pores is an important component of dialyzers which clean blood from contaminations in case of renal insufficiency.

4. INNOVATIVE METHOD OF SEPARATING BLOOD INTO COMPONENTS WITH THE USE OF ULTRASOUNDS

Ultrasounds are mechanical waves (elastic waves) of frequency higher than 20 kHz with the upper limit of 10 GHz. The range of frequency of different elastic waves is presented in Fig. 2.

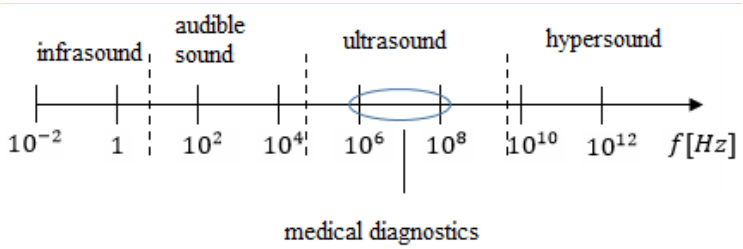

Fig. 2. Frequency range of ultrasound used in medical diagnostics.
Own elaboration based on [8]

The effects of ultrasound are divided into passive and active. Passive use of ultrasound consists in the use of ultrasound wave of low intensity that does not destroy the wave bearing medium. Passive effects of ultrasound waves are used in medical and technical diagnostics.

Active ultrasound involves the use of waves of medium and high intensity. Such waves cause chemical, biological and physical changes of a medium in which they are spread out. Active effects of ultrasound cause irreversible changes of the medium and are used, for instance, in medical therapy. Media in which waves are spread out may be divided into two groups: ideal and real ones.

In ideal (lossless) media there is no attenuation of waves whereas in the real ones the waves are absorbed. Due to heterogeneity of real media the waves are dispersed. Such heterogeneity may result from contaminations, defects in structure or internal stress. If attenuation is low, it might be ignored and the medium may be treated as an ideal one.

Dispersion of ultrasound in blood is (in some approximation) proportional to the hematocrit[3] and to frequency. The main source of dispersion of ultrasound energy in the frequencies ranging from 4 to 16 MHz are erythrocytes [9]. Energy of a wave of frequency of 5 MHz dispersed in platelets is about 1000 times lower as compared to the energy dispersed in erythrocytes [9].

Table 2 includes different velocity values of ultrasound waves spread out in plasma and blood. The ratio of density of medium and velocity of waves spread out in this medium is known as acoustic impedance [9]:

$$Z = \rho_0 c = \sqrt{\rho_0 B_{ad}} \tag{7}$$

In the above equation it is considered that $c = \sqrt{\frac{B_{ad}}{\rho_0}}$, where B_{ad} – adiabatic elasticity coefficient.

[3] For HCT lower than 40%. For HCT = 45% and frequency of 5 MHz absorption equals 0.8 dB/cm [9].

Wave incident on media with different acoustic impedance undergoes a partial reflection. Table 2 presents acoustic properties of blood [9].

Table 2. Acoustic properties of blood. Source [9]

Medium	**Density ρ [kg·m^{-3}]·10^3**	**Impedance Z [kg·m^{-2}·s^{-1}]·10^6**	**Velocity c [m s^{-1}]**
Blood	1.06	1.66	1570
Erythrocytes	1.091	1.55	1590
Plasma	1.021	1.73	1520
Water	0.998	1.49	1500

5. CHANGES IN CONCENTRATION OF BLOOD COMPONENTS IN PLASMA IN AN ULTRASONIC STANDING WAVE FIELD

Red blood cells suspended in plasma are characterized by significant mobility. Ultrasound wave that is spread out in a fluid medium not only causes vibration but also progressive movement of particles [10]. As a result, movement of particles that are suspended in such medium is a sum of rapid vibrating movement and slow progressive movement towards the medium [11].

While exposing blood to standing ultrasound wave, changes in concentration of solid particles i.e. erythrocytes suspended in plasma are observed in the area between node and antinode of a wave [12, 13].

While $N = N(x,t)$ denotes number of particles per volume unit in a surface described by coordinate x at a time t, continuity equation is expressed as follows [14]:

$$N(x,t) = \frac{N_0}{\sin^2 kx \exp(-\partial t) + \cos^2 kx \exp(\partial t)} \tag{8}$$

where: $\delta = 2kv_D$; v_D – velocity of progressive movement of erythrocyte; k – wave number; N_0 – initial concentration of erythrocytes; δ^{-1} – time constant of concentration of erythrocytes.

Equation (8) indicates that there are changes in concentration of erythrocytes in the standing wave field. Concentration of erythrocytes in antinodes and nodes of standing wave changes exponentially. Erythrocytes are filtered out from the areas where concentration increases in accordance with the relationship $N_0 e^{\delta t}$. As shown by calculations [11] an increase in concentration of several hundreds of thousands times is achieved as compared to the initial concentration within fractions of a second.

REFERENCES

[1] Jóźwiak Z., Bartosz G., *Biophysics*, Warsaw 2005.

[2] Sliwiński A., *Ultrasounds and their applications*, Warsaw 2003.

[3] Sadikova D.G., Andreev A.A., Shkidchenko A.N., Pashovkin T.N., *Dynamics of Cells Concentration in a Standing Ultrasonic Wave*, Biomedical Technology and Electronics, 2006, 8-9, pp. 95-99.

[4] Sadikova D.G., Pashovkin T.N., *Cell concentration and separation in the field of a Standing Ultrasonic Wave for Medicine and Biotechnology*, Open Journal of Biophysics, 2013, 3, pp. 70-75.

[5] Ziolko E., *Fundamentals of human physiology*, Nysa 2006.

[6] Rajzer M., Palka I., Kawecka-Jaszcz K., *The importance of blood viscosity in the pathogenesis of hypertension*, Krakow 2014.

[7] Ceynowa J. et al., *Membranes theory and practice*, Torun 2003.

[8] Pietrzak M., Ibhron G., Wieczorek Z., *Physical basis of ultrasounds application in medicine*, Olsztyn 2011.

[9] Nowicki A., *Ultrasounds in Medicine*, Warsaw 2010.

[10] Trampler F., Schwartz D., Mayr W., Benes E., *Purification of platelets in human blood by means of ultrasonics*, Proc. WCU 97, 1997, Yokohama, Japan, pp. 24-27.

[11] Czyz H., Jasinski T., Wloch A., *Distribution functions and time constants of the process of cell concentration changes in bodily fluids in the field of ultrasonic standing wave*, Archives of Acoustics, 2017, 42, 3, p. 543.

[12] Pashovkin T.N., Sadikova D.G., *Cell Exfoliation, Separation, and Concentration in the Field of a Standing Ultrasonic Wave*, Acoustical Physics, 2009, 55, 4-5, pp. 584-593.

[13] Pashovkin T.N., Sadikova D.G., Pashovkina M.S., Shilnikov G.V., *The Use of Ultrasonic Standing Wave in Biological Research and Cell Technologies*, Bulletin of Experimental, Biology and Medicine, 2007, 3, pp. 133-138.

[14] Wloch A., Czyz H., Jasinski T., *Ultrasonic methods of the cells separation in human blood*, Acta Physica Polonica A, 2015, pp. 234-236.

FIZYKA W MEDYCYNIE I GOSPODARCE WSPÓŁCZESNEGO SPOŁECZEŃSTWA

Współczesne społeczeństwa są świadome znaczenia odkryć fizycznych dla gospodarki i medycyny. Nasze codzienne życie jest silnie związane z urządzeniami technicznymi, które zostały wytworzone na podstawie fundamentalnych praw fizyki. W pracy analizowano fizyczne metody rozdzielania krwi ludzkiej na składniki. Obecnie w praktyce medycznej najczęściej stosowanymi metodami są wirowanie i filtracja. Dokonując analizy podstaw fizycznych metod tradycyjnych separacji krwi na składniki, zaprezentowano także innowacyjną metodę, która wykorzystuje fale ultradźwiękowe o parametrach dobranych do parametrów składników krwi. Metoda ta jest teoretycznie opracowana, wymaga natomiast weryfikacji eksperymentalnej w celu wdrożenia jej w diagnostyce medycznej.

Słowa kluczowe: prawa fizyki, ludzka krew, separacja krwi ludzkiej, wirowanie, filtracja, akustyczna fala stojąca, medyczne zastosowania ultradźwięków

Received: 18.10.2017
Accepted: 13.11.2017

Paulina KALAMARZ[1]
Magdalena ZAGROBELNA[2]
Leszek PYZIAK[3]

FOCUSING ULTRASOUNDS BEAM

The focused ultrasound beam is very important in diagnostics and medical treatments. The aim of the study is to analyze the basic physical phenomena in the process of focusing the ultrasonic wave. Based on the measured temperature in the focus of the ultrasonic beam. The compatibility of the temperature measurement by the method HIFU optical fiber.

Keywords: ultrasounds, focus ultrasound beam

INTRODUCTION

Sound is a physical phenomenon that transmits acoustic energy from one point to another. It differs from the electromagnetic radiation that the sound can propagate only in the elastic environment. It does not pass through a vacuum, just like electromagnetic radiation. One of the most important physical qualities of sound is the frequency – speed, with which the source of the sound vibrates. The human ear does not react to all frequencies. The range of human audible frequencies is from 20 Hz to 20 000 Hz (20 kHz).

Ultrasound – the spring waves, with frequencies above 20 000 Hz, covering a wide, compared to the audible, frequency range. Low frequency ultrasound (in the range of tens of kHz) produces and recognizes many animals such as dogs, cats, bats, and dolphins [1]. Thanks to its properties, ultrasounds have wide applications. Depending on the intensity, ultrasound is used for: materials testing, structural strength, and tracking of non-observable processes by other methods.

In medicine ultrasound helps in diagnostics and treatments. They help to monitor the progress of treatment. Wide diagnostic has got ultrasonography.

[1] Corresponding author: Paulina Kalamarz, student, Rzeszow University of Technology, Powstancow Warszawy 8, 35-959 Rzeszow, Poland, phone: (17) 8651744, e-mail: paulina.kalamarz@op.pl
[2] Magdalena Zagrobelna, Rzeszow University of Technology, e-mail: magdalena.zagrobelna@op.pl
[3] Leszek Pyziak, Rzeszow University of Technology, e-mail: l.pyziak@prz.edu.pl

1. CONSTRUCTION OF THE ULTRASOUND HEAD

Ultrasounds can be used to obtain a lot of information from the inside of the body and to the thermoablation. To obtain an ultrasound image, the transducer must be able to transmit and receive ultrasonic waves, and should be able to focus the beam reaching the tissue. The ultrasound head (Fig. 1) is the basic part of ultrasound. This is an important element because without which it, to watch images of the interior of the organism on the computer screen would be impossible. The correct operation of the head depends on the end of the crystal tip of the head with the tissue. Incorrect coupling results in deterioration image quality. The lack of any coupling can cause damage to the head, because all of the wave energy is converted to heat, in small volumes, near the end of the transmitter element [2].

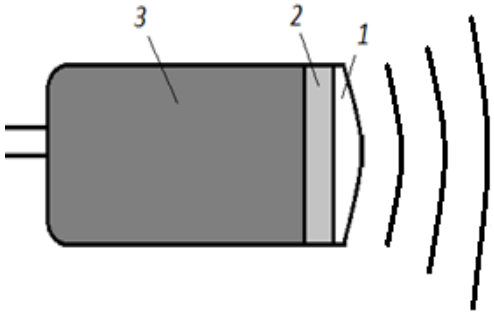

Fig. 1. Ultrasonic head: 1 – impedance transformer,
2 – piezoelectric transducer, 3 – damping material [2]

The main components of the head include:

- **damping material** – which is usually epoxy resin mixed with tungsten powder – provides an acoustic impedance equal to the impedance of the crystal;
- **piezoelectric crystals** – they show piezoelectric effect, consisting of appearing on his surface of electrical charges under the influence of mechanical stresses;
- **impedance transformer** – is responsible for the smooth transition of the wave ultrasonic by tissue.

One of the important parameters determining the quality of imaging ultrasound is the **resolution**, the ability to distinguish closely-spaced structures that differ in properties. The narrower the beam, the easier it will be to distinguish echoes reflected from different tissues. In order to improve image quality, ultrasound beam focusing is used. It can be received by:

- **mechanical (structural)** – using the shape of piezoelectric transducer. The disadvantage of such beam focus is that it is focused only at one point.

This can be a hindrance when there is a need to observe larger objects in the whole field of view;

- **electronic** – it is much better than construction since it allows the beam to be focused throughout the field of vision. This is possible with the delay lines [3].

Ultrasonic delay lines are systems that to slow down an electrical signal (moving at the speed of an electromagnetic wave) they process the signal on ultrasonic (about 10^5 times slower than electrical) and then transform it into an electrical signal. Delay time depends on the length of the ultrasonic path and may range from microsecond fractions to tens of milliseconds [1].

2. PIEZOELECTRIC TRANSDUCER

The piezoelectric transducer is made up of tiny crystals that are several millimeters' length and width corresponding to the thickness of the hair (Fig. 2). He's full alternating two functions: **transmitting** (produces ultrasonic pulses) and **receiving** (detection of returning echoes) [4].

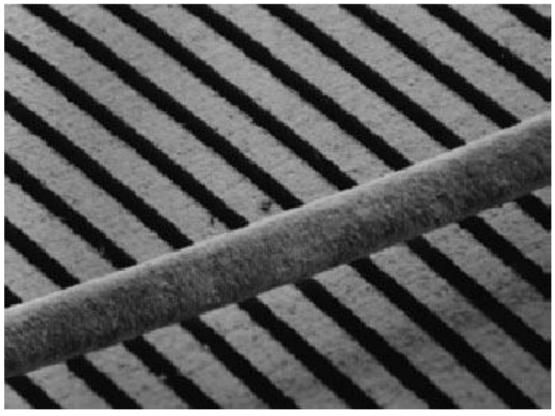

Fig. 2. Piezoelectric transducer. In the foreground, there is a human hair [5]

We can also control each crystal separately, we can emit and receive ultrasounds depending on the element. The transmitter also concentrates the pulse beam to give a specific shape and size at different depths throughout the body and also scans the radius of the anatomical area that is mapped.

The size of the transmitter determines the resonance frequencies of vibration. Assuming that one surface of the tile is firmly bound to the damping material and the other surface is in contact with a material with a much lower acoustic impedance that can be considered free, then by dependence (1):

$$v_{2n-1} = (2n-1)\frac{c_p}{4l} \tag{1}$$

where: c_p – the velocity of the acoustic wave in a direction perpendicular to the surface; $n = 1,2, ...$; l – thickness of the piezoelectric plate

We can calculate the thickness of the piezoelectric plate for the resonance frequency. For example, for a tile made of zirconate-lead titanate – **PZT** and a frequency of 1 MHz the thickness is 0,63 mm [6].

The capacitance of the transmitter results from its design. Each transmitter has a maximum permissible value of alternating supply voltage. This is due to the risk of mechanical damage due to vibration. If the transmitter is energized with too high alternating voltage, the deformation and stress of the element will be so great that the item will be severely damaged.

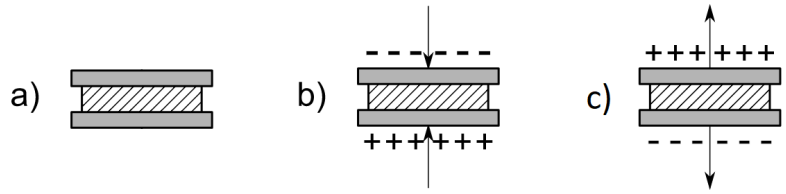

Fig. 3. Piezoelectric effect in quartz crystal SiO_2: a) crystal in equilibrium, b) compression crystal, c) crystal extended [7]

Ultrasonic transducers are built of crystals that contain electrical dipoles in the crystal lattice. Deformation of the crystal lattice is related to piezoelectric properties. The piezoelectric crystal in equilibrium does not show the presence of electrical charges. After its mechanical deformation, its spatial density of charge is impaired and electrical charge is generated on the surface of this crystal (Fig. 3) [8].

A crystal of thickness x is set to wave length generation: $\lambda = 2x$ and frequency: $f = \frac{c}{\lambda}$. The cycle of this wave is: $T = \frac{1}{f} = \frac{2x}{c}$. If the probe is to produce as short a pulse as possible, the crystal is stimulated with a rectangular pulse of time T_{imp} (2) [8]:

$$T_{imp} = \frac{1}{4}T = \frac{x}{2c} \tag{2}$$

The crystal in the piezoelectric transducer deforms under the electric field and its surface performs a $\frac{1}{4}$ sinusoid motion. Then, when the stimulus pulse ends, the crystal returns to balance (Fig. 4). At the moment of equilibrium, the surface of the crystal has made an appropriate movement of the sinusoidal half. Stored in

the crystal the kinetic energy will cause further crystal oscillations of increasing less amplitude. The quality of the damping material influences how quickly these vibrations expire [8].

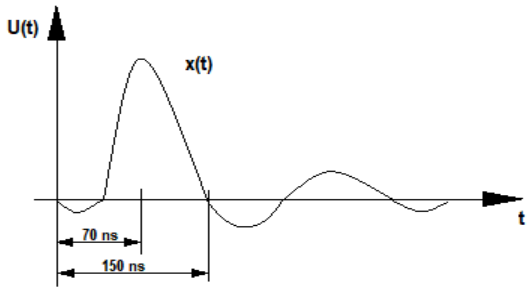

Fig. 4. Impulse stimulation and transducer vibration [8]

Each point of the oscillating crystal is the source of the spherical wave, transmitted at the broadcasting center. For this reason, numerous interferences occur near the transducer. The field in which interference occurs is called a **close field**. On the other hand, the area in which the mechanical wave spreads uniformly, without interference, is called a **far field** [8].

The range of the near field depends on the diameter of the transducer and on the frequency of the ultrasonic wave [8] defined by the formula (3):

$$x_n = \frac{d^2 \cdot f}{4c} = \frac{d^2}{4\lambda} = \frac{r^2}{\lambda} \tag{3}$$

where: x_n – range of near field; d – transducer diameter; r – transducer radius; f – wave frequency; λ – wavelength; c – velocity of wave propagation.

At the boundary of the near and far field there is a small concentration of the wave, called the ultrasonic beam itself (Fig. 5).

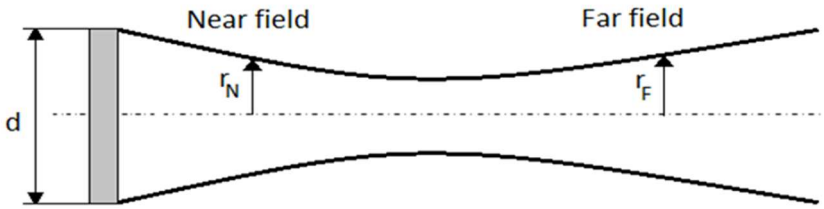

Fig. 5. Near field, far field, and beam self-focusing [8]

The width of a beam can be represented by the relationships (4) and (5) [8]:

- in the near field:

$$2r_N = 2r - \frac{\lambda \cdot x}{r} \tag{4}$$

- in the far field:

$$2r_F = \frac{\lambda \cdot x}{r} \tag{5}$$

where: d – transducer diameter; r – transducer radius; x – distance from transmitter; λ – wavelenght.

3. ELECTRONIC FOCUS OF THE ULTRASOUND BEAM

Focusing on the transmitter can be changed electronically when it is in echo reception mode. Knowing the location of the point A and the velocity of the wave (Fig. 6) you can determine the time taken by the wave moving from point A to transmitter elements (crystals). This is accomplished by processing electrical pulses from individual transducer elements for various time delays before they are combined into one electrical pulse. In this way, the effect of focusing echoes is created.

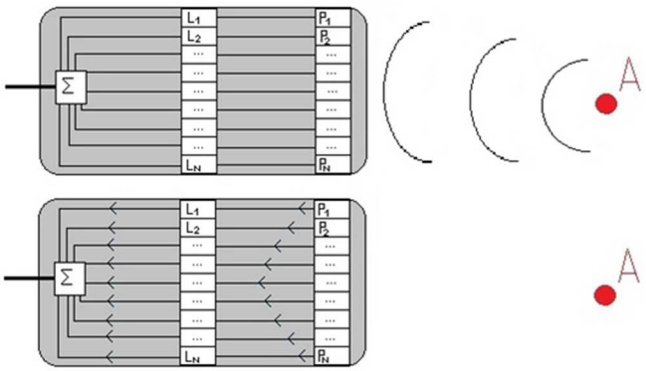

Fig. 6. Scheme of ultrasonic wave reception
(P – transducer, L – delay line) [5]

This phenomenon also works in the opposite direction (Fig. 7). An electric impulse can be applied to the delay line where the pulse is released at different speeds to form a wave. In this way, we will also receive a focused beam, because in the end the ultrasound waves due to interference will be reflected in point A.

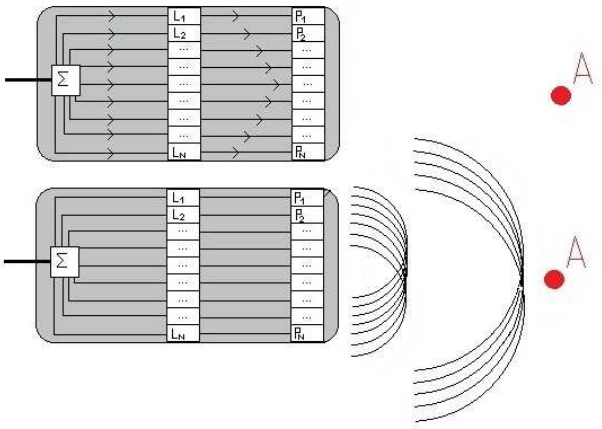

Fig. 7. Scheme of beam focus at point A (P – transducer, L – delay line) [5]

This kind of focus gives flexibility in creating beams of various shapes and sending the beam in any direction. The described dynamic focus is a major achievement that allows the tissue to be examined without moving the probe.

4. MECHANICAL METHODS OF FOCUSING ULTRASONIC BEAM

The focus beam can also be obtained by using, as in optics, focusing lenses. While in optics, convex lenses are used for this, ultrasonography uses concave lenses. This is due to the properties of the material from which the lenses are manufactured, because the ultrasonic velocity in the ultrasonic lenses is greater than in the tissue [9].

The effect of focusing with ultrasonic lenses is related to the law of refraction of waves at the border of two centers (Fig. 8). According to the laws of Snellius (6) we have:

$$\frac{\sin\alpha}{c_1} = \frac{\sin\beta}{c_2} \tag{6}$$

after transformation:

$$\sin\alpha = \frac{c_1}{c_2}\sin\beta = n\sin\beta \tag{7}$$

when $n = \frac{c_1}{c_2}$ – refractive index.

The position of the F point can be calculated using the trigonometric relationships:

$$AB = R\sin\alpha = f\sin(\alpha - \beta) \tag{8}$$

For small angles $\alpha\ i\ \beta$, and $s < 0{,}1R$, sines of angles can be approximated by the values of these angles. Similarly, in optics, and after transforming the equation (8), we obtain the pattern (9) for the location of the focus:

$$f = \frac{R\alpha}{\alpha-\beta} = \frac{Rn\beta}{n\beta-\beta} = \frac{R}{1-\frac{1}{n}} \tag{9}$$

Depending on the study, the ultrasonic heads are focused at different depths, eg in obstetrics and abdominal studies, ranging from a few to several centimeters, in cardiology for cardiac tests of 5-10 cm, and in angiography 1-2 cm [9].

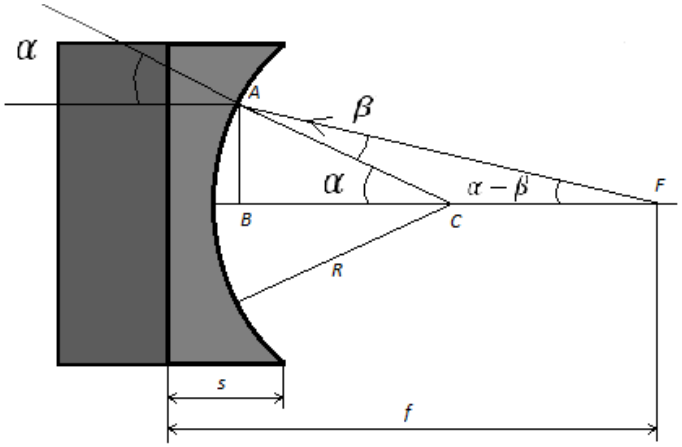

Fig. 8. Principle of focusing ultrasonic beam
(R – lens curvature radius, f – focal length) [9]

5. HIGH INTENSITY FOCUSED ULTRASOUND METHOD IN THERMOABLATION AS ONE OF THE APPLICATIONS OF THE ULTRASONIC BEAM

One example of the use of a spherical ultrasonic beam is thermal ablation. There have been many attempts to develop operations using high-power ultrasonic beams. This non-invasive method of medical treatment was very attractive, but technically out of reach because of the lack of reliable and effective methods of temperature monitoring [10]. Significant technical progress in magnetic resonance imaging enabled temperature monitoring and ultrasound operations (Table 1).

Table 1. Properties of Philips Sonavelle system [10]

Parameters of Philips Sonavelle HIFU System	
Therapy time	1-4 h
Sonication time	10-75 s
Max sonication power	250 W
Ultrasound frequency	1,2-1,4 MHz
Power intensity	500-5000 W/cm^2
Focus size	1.5 x 1.5 x 10 mm
Spot sizes diameter	4/8/12/16 mm

Magnetic resonance magnetic resonance spectroscopy, the stimulation of nuclear spins in the outer magnetic field by rapid changes in the magnetic field causes the recording of electromagnetic radiation by relaxation phenomena. Therefore, the temperature measured by this method achieves an accuracy of ± 1°C.

There is a linear relationship (10) between the change in the frequency of the proton vibrations and the increase in temperature. The temperature rise is calculated from the phase differences based on the formula:

$$\Delta T = \frac{\Delta\varphi}{\alpha\gamma B_0 t_e 2\pi} \tag{10}$$

where: γ– gyromagnetic ratio – 42,58 MHz/T; α – temperature dependent water resonance chemical shift 0,0094 ppm/°C.

The PRF of the lipid hydrogen is temperature independent, therefore the temperature

The fat tissue cannot be measured with a MR thermometer.

The HIFU method is used to treat uterine fibroids, palliative bone pain treatment, prostate cancer, and breast cancer [10].

The disintegration of uterine fibroids occurs through sonication, which is the use of ultrasonic energy inside the body. During intervention, the beam of ultrasonic energy penetrates the skin and soft tissues, causing the temperature to rise in a particular area. A thrombotic necrosis area is produced within a few seconds. Therefore, the extent to which the tissues are exposed to temperature increase and the polystyrene plate could be used to protect the affected areas [11].

For this purpose, in the experiment were used:

- biological material – vein tissue;
- fiber optic sensor FOT-M;
- one-channel interface FTI-10 from FISO.

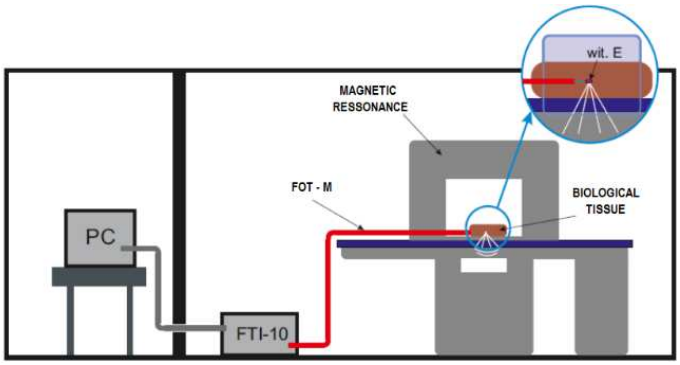

Fig. 9. Diagram of the measuring system [11]

At the beginning, the muscle was heated to 35°C to be close to to human body temperature. Below this temperature, the software does not allow for the surgery. Then the tissue is placed inside the magnetic resonance. Inside the room was a sensor with an interface, the sensitivity zone of the sensor was inside the muscle. Also, a vitamin E capsule was placed at the sensitivity of the sensor, which acted as a marker for imaging the sensor by resonance. Also used was the polystyrene plate that was placed behind the focus of the ultrasonic beam. The remaining equipment was located in a separate room (Fig. 9).

Measurements have been made several times. It also succeeded get a denaturation temperature of the protein. There was no cavitation, so we were able to perform the ultrasonic thermoablation treatment properly. The results are presented in Fig. 10.

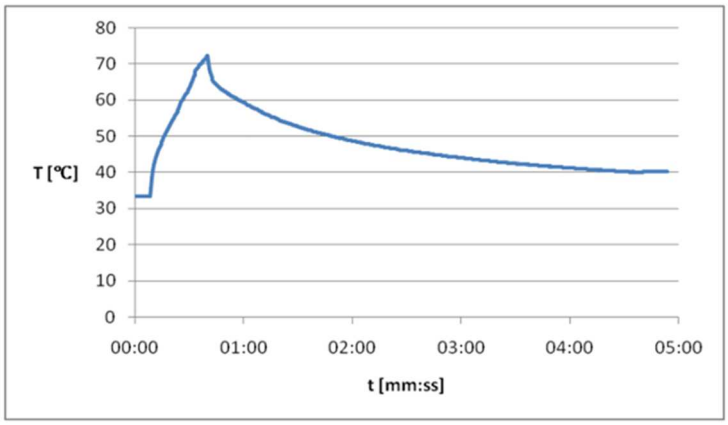

Fig. 10. Dynamics of changes in biological tissue temperature [11]

Plate measurements were also performed inside the muscle tissue. Figure 11 shows the scheme of operation of the system used on the board. It has been verified that it can be used as a manipulator. The measurement results are shown in Fig. 12.

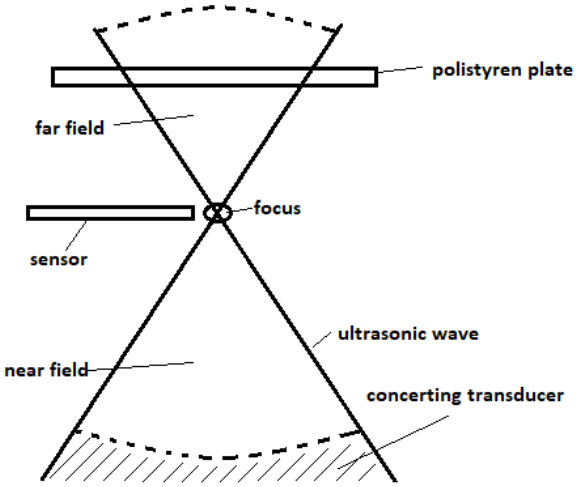

Fig. 11. Philips Sonalleve system diagram for polystyrene board [11]

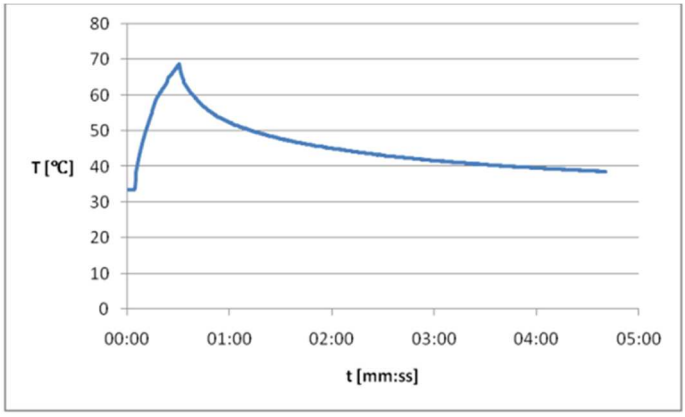

Fig. 12. Dynamics of temperature changes of biological tissue covered by polystyrene plate [11]

As it turned out, the tile was destroyed during the research and therefore could not be used as a manipulator.

6. CONCLUSIONS

Focusing of the ultrasonic beam can be realized by mechanical (structural) and electronic methods. In case of thermoablation, mechanical focusing is used. In the focal point an increase in the power density of the ultrasonic beam is obtained in the absence of cavitation. Achieving a temperature of 70°C set as a parameter in the HIFU was confirmed by the fiber optic sensor used in the measurements. In the case of placement from the polistery plate behind the ultrasonic wave, structural damage has been observed.

REFERENCES

[1] Śliwiński A., *Ultradźwięki i ich zastosowania*, Wydawnictwa Naukowo-Techniczne, Warszawa 1993, 2001.

[2] Augustyniak P., *Elektroniczna aparatura medyczna*, Wydawnictwa AGH, Kraków 2015.

[3] www.scribd.com/document/308359371/ULTRASONOGRAFIA.

[4] http://www.sprawls.org/ppmi2/USPRO/ (available: 4.03.2017).

[5] www.futurelearn.com/courses/ultrasound-imagining/0/steps/10292 (available: 4.03. 2017).

[6] Hrynkiewicz A.Z., Rokita E., *Fizyczne metody diagnostyki medycznej i terapii*, Wydawnictwo Naukowe PWN, Warszawa 2013.

[7] https://pl.wikipedia.org/wiki/Piezoelektryk (available: 5.03.2017).

[8] Padee L., *Aparatura ultrasonograficzna*, wykład, Wydział Elektroniki i Technik Wytwarzania, Politechnika Warszawska.

[9] Nowicki A., *Ultradźwięki w medycynie wprowadzenie do ultrasonografii*, Wydawnictwo Instytutu Podstawowych Problemów Techniki, PAN, Warszawa 2010.

[10] Wolski S., Trybus M., High Intensity Focused Ultrasound therapy under magnetic resonance control, AMPERE NMR School, Zakopane 2015.

[11] Zagrobelna M., *Pomiar temperatury interferometrycznym czujnikiem światłowodowym i jego zastosowania*, Praca inżynierska, Rzeszów 2016.

OGNISKOWANIE WIĄZKI ULTRADŹWIĘKOWEJ

Ogniskowana wiązka ultradźwiękowa ma bardzo ważne znaczenie w diagnostyce i zabiegach medycznych. Celem pracy jest analiza podstawowych zjawisk fizycznych w procesie ogniskowania fali ultradźwiękowej. Na podstawie przeprowadzonego pomiaru temperatury w ognisku wiązki ultradźwiękowej stwierdzono zgodność pomiaru temperatury metodą HIFU z metodą światłowodową.

Słowa kluczowe: ultradźwięki, ogniskowanie ultradźwięków

Received: 6.10.2017
Accepted: 20.10.2017

Marzena MALICKA[1]
Mateusz MALICKI[2]

MEASUREMENT OF THE INTENSITY OF THE ELECTRIC FIELD OF THE RADIO WAVE EMITTED BY SELECTED MOBILE PHONES

We are constantly watching the growth of mobile phone users around the world. This causes interest in the issue of the influence of electromagnetic radiation on the human body. The sources of electromagnetic fields are among others mobile telephony. Mobile telephony consists of two basic elements: telephones (terminals) and base stations. Specific Absorption Rate (SAR) means the unit of amount of radiofrequency energy absorbed by the human body when using a mobile phone. The aim of the study was to measure the intensity of the electric field of the radio wave emitted by selected mobile phones. The measurements were carried out in the Radiation Measurement Laboratory at the Provincial Sanitary-Epidemiological Station in Rzeszów. Measurements were made for devices operating in different data transmission systems operating in certain frequency bands. The electric field of the electromagnetic field was measured using an wide field electromagnetic field measuring device type NBM-550 No. B-0240 with EF-1891 type probe. Measurements were made for devices with switched on and off data transmission at the time of receipt and during signaling. In the following sections describe mobile telephony and the basic characteristics of the mobile phone technology. The last part presents the way of making measurements and presentation of results.

Keywords: electromagnetic field, mobile telephony, base stations, Specific Absorption Rate (SAR)

INTRODUCTION

Today we are constantly exposed to many negative factors between other electromagnetic radiation. Natural electromagnetic radiation is the result of cosmic and atmospheric phenomena. Artificial electromagnetic radiation comes from industrial and everyday equipment. The sources of electromagnetic fields are

[1] Corresponding author: Marzena Malicka, Rzeszow University of Technology, Powstancow Warszawy 8, 35-959 Rzeszow, Poland, phone: (17) 8651744, e-mail: m.malicka@prz.edu.pl
[2] Mateusz Malicki, Provincial Sanitary-Epidemiological Station in Rzeszów, e-mail: mateusz.malicki@wsse.rzeszow.pl

power lines, radio and television stations, Internet access stations and mobile telephony. The electromagnetic field is an electric, magnetic and electromagnetic field with frequencies from 0 to 300 GHz (according to Article 3 point 18 of the Environmental Protection Law). The electromagnetic field is described by: field power density (W/m^2), intensity of the electric field (V/m), and the intensity of the magnetic field (A/m) [1].

Currently, there are as many as 4.92 billion unique mobile users in the world – 66% of the population – and 8.05 billion active SIM cards - that means 1.64 of a single user. Poland is ranked 17th in terms of penetration of mobile users – as many as 74% of our people use mobile phones. Spain (88%), Singapore, Italy and Japan (85%), followed by Germany (82%). Data based on a detailed report on the state of the Internet, mobile and social media in the world in 2017.

1. MOBILE TELEPHONY

Mobile telephony is a telecommunications infrastructure that enables subscribers to wirelessly connect to a cellular area controlled by individual base station antennas. A characteristic feature of this type of telephony is to provide the user with mobility. It can set up calls in the radio coverage area associated with all base stations on the network. The world's largest mobile telephony system is GSM-second-generation mobile telephony (about 80% of the mobile telephony market). In 2001 the first commercial telephony network was launched. Among the world's most deployed 3G systems, most networks (73%) are built on the UMTS (Universal Mobile Telecommunications System) standard. The successor of the third generation is the wireless data transmission standard is Long Term Evolution (LTE). The main goals of the new standard are, among other things, increasing the capacity of mobile telephony by increasing the speed of data transmission, reducing delays.

Mobile telephony consists of two basic elements telephones (terminals) and base stations. According to data from the Office of Electronic Communications in Poland there are 45.5 thousand base stations. Currently the most common sources of artificial electromagnetic fields are cellular base stations. Cellular base stations consist of sector antennas and radio antennas. The sectoral antenna is responsible for communicating with the mobile phone, and the radio antenna for communication between the base stations [2]. Table 1 shows examples of electromagnetic field sources and their corresponding frequency ranges.

The main principles of protection of people at the workplace against nonionizing electromagnetic radiation are defined among others in the Regulation of the Minister of Family, Labor and Social Policy of 29 June 2016 (Item 950).

Mobile base stations are designed so that the average field power density values that could exceed the allowable level are concentrated at high altitudes. Due to the increase in mobile phone users, base stations are designed for multisystem operation. In addition, according to the Law of Environmental Protection,

it is mandatory to obtain a permit to emit electromagnetic fields into the environment without which the newly constructed investment or the object can not be put into use [3].

Table 1. Sources and frequency ranges of emitted electromagnetic fields (Military Institute of Hygiene and Epidemiology Volume 35, Supplement 2)

Description of the magnetic field	**Frequency range**	**Wavelength**	**Sources and circumstances of occurrences of fields**
Static magnetic and electromagnetic fields	0	-	electric motors, electrolysis and industry
(AC) grid network fields	50 or 60 Hz	6000 or 5000 km	electrical power, lighting, heating, engines, power supply and industry
Very low frequency fields	0,1-1,0 kHz	300-3000 km	industrial equipment
Low frequency fields	1-100 kHz	3-300 km	industrial equipment
Radio waves	0,1-300 MHz	1-3000 m	radiophony, radiotelephones, medical devices
Microwaves	0,3-300 GHz	1-1000 mm	radiolocation, radionavigation, mobile telephony, medical devices, home and industrial appliances

The electromagnetic field emitted by mobile phones depends on the type of phone, the distance from the base station, the phase of the call. Maximum field values are dialed and their value decreases during the call [4]. Due to the dynamic development of mobile telephony, various data transmission systems have been developed, including those operating at frequencies of 900 MHz, 1800 MHz, 2000 MHz and 2100 MHz.

2. PERFORMING MEASUREMENTS

The experiment consisted in checking the indication of electrical component of the electromagnetic field intensity emitted by selected smartphones and one mobile phone. Measurements were made for devices operating in different data transmission systems operating in certain frequency bands. The measurements were carried out in the Laboratory of Radiation Measurement in the Provincial Sanitary-Epidemiological Station in Rzeszów. The electric field of the electromagnetic field was measured using an wide field electromagnetic field measuring device type NBM-550 No. B-0240 with EF-1891 type probe. The meter and the probe are attached to a tripod. On the second stand, the device was placed just below the probe. The distance between the probe and the head of the test source

was determined by means of a measuring tape. The distance between the measurements was constant and was 4 cm. Measurements were made from the front of the phone (Fig. 1, Fig. 2).

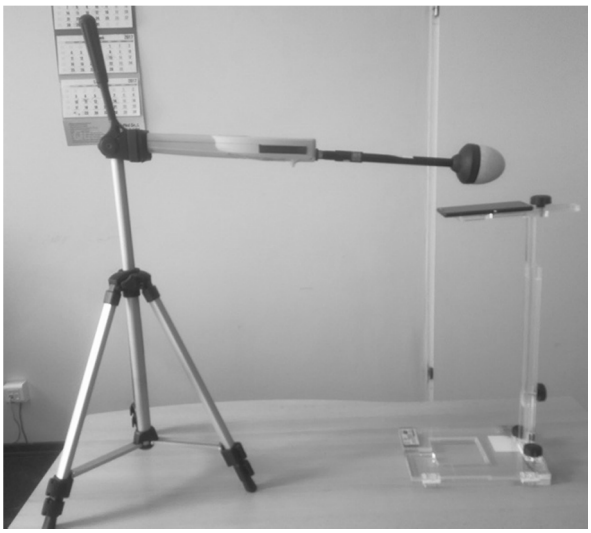

Fig. 1. Method of measurement (side view)

Fig. 2. Method of measurement (top view)

Measurements were made for 5 different smartphones and one mobile phone. During the experiment the phones range was maximal. The average results of electrical component of electromagnetic field measurements based on the ten readings are summarized in Table 2. Measurements were performed with data switched on and off while receiving and during signaling.

Table 2. Measurement of electrical component of electromagnetic field for selected devices

Device type	Data transmission technology	Measurement with data enabled, V/m		Measurement without data transmission, V/m	
		during signaling	at the time of recept	during signaling	at the time of recept
Smartphone 1	LTE	<0,5*	<0,5*	0,56	<0,5*
Smartphone 2	LTE	<0,5*	<0,5*	<0,5*	<0,5*
Smartphone 3	LTE	0,83	0,95	0,89	0,98
Smartphone 4	HSDPA	<0,5*	<0,5*	<0,5*	<0,5*
Smartphone 5	LTE	0,95	1,43	0,72	0,63
Mobile phone	–	–	–	15,9	5,7

* indication below the detection limit of the meter according to the calibration certificate of the device.

The results shown in Table 2 read directly from the meter were corrected according to the calibration certificate of the device according to the formula:

$$\mathrm{Ecor} = \mathrm{Em} \cdot \mathrm{Cd} \cdot \mathrm{Cf} \tag{1}$$

where: Ecor – corrected value; Em – measured value; Cd – dynamic characteristics; Cf –frequency characteristics.

According to the calibration certificate, results ranging from 0,5 to less than or equal to 0.75 V/m were corrected for correction factor (Cd · Cf) 1.05. Values in the range of greater than 0.75-1.5 V/m were corrected for a correction factor of 1.09. Values in greater than 0.75-1.5 V/m were corrected for a correction factor of 1.09. The calculated values are shown in Table 3.

Table 3. Measurement results after correction with correction factors

Device type	Data transmission technology	Measurement with data enabled, V/m		Measurement without data transmission, V/m	
		during signaling	at the time of recept	during signaling	at the time of recept
Smartphone 1	LTE	<0,5*	<0,5*	0,59	<0,5*
Smartphone 2	LTE	<0,5*	<0,5*	<0,5*	<0,5*
Smartphone3	LTE	0,91	1,04	0,97	1,07
Smartphone 4	HSDPA	<0,5*	<0,5*	<0,5*	<0,5*
Smartphone 5	LTE	1,04	1,56	0,76	0,66
Mobile phone	-	-	-	18,3	6,3

After analyzing the results of the measurements in Table 3, it is concluded that most of the measured values for smartphones oscillate around 0.5 to 1.56 V/m.

Measurements for cellular phones gave values of 18.3 V/m during connection and at the time of recept of 6.3 V/m.

During the measurements for all devices, a momentary increase in the electromagnetic field (about one second) to 2.5 V/m was observed at such phases as the start of the connection and at the time of recept. This can be explained by the fact that when making a call, the phone transmits for a short while with a power close to the maximum. When the connection is established, the signal parameters are adjusted to the reception and transmission conditions and the signal strength is reduced. It is recommended that you wait a while before applying the telephone to your ear [5].

3. CONCLUSIONS

During a call the phone is usually kept close to the head, so measurements are taken at a distance of 4 cm. Due to the construction of the probe, it was not possible to carry out measurements at a closer distance.

In order to limit the impact of mobile phones, you can use certain recommendations such as:

- increasing the distance between the head and the mobile phone,
- use headset and handsfree with internal or external antenna in your car,
- shortening talk time,
- avoid making calls away from base stations, turning off phones where there is no coverage (in the absence of coverage, it will attempt to connect to the base station, acting with full power of the transmitter),
- you can move closer to the window when the call is in progress so that the transmitter and base stations can work with less power.

Electromagnetic radiation from cell phones and base stations is not indifferent to human health. Negative effects depend on the absorbed value of the electromagnetic energy and the resistance of the body [6].

It is certain that every cell phone emits radiation. Therefore, choose a model that has the lowest SAR value. Specific Absorption Rate (SAR) means the unit of amount of radiofrequency energy absorbed by the human body when using a mobile phone. EU law requires the SAR value for each mobile phone to be given in Europe – this value can not be higher than 2 W/kg.

The SAR is difficult to determine and may be estimated for example by measurements of the electric field strength of the radiation, the temperature increase or by numerical simulations [7, 8].

REFERENCES

[1] Różycki S., *Ochrona środowiska przed polami elektromagnetycznymi. Informator dla administracji samorządowej*, Generalna Dyrekcja Ochrony Środowiska, Warszawa 2011.

[2] http://www.wios.warszawa.pl/pl/monitoring-srodowiska/monitoring-pol-elektro/zrodla-promieniowania/78,Zrodla-promieniowania-elektromagnetycznego.print (available: 03.11.2017).

[3] Michałowska-Samonek J., *Aktualne zasady dotyczące badania pól elektromagnetycznych wysokiej częstotliwości*, Prace Instytutu Elektroniki, 2008, z. 238.

[4] Zmyślony M., Politański P., *Zagrożenia zdrowia i ochrona zdrowia pracujących w narażeniu na pola i promieniowanie elektromagnetyczne 0-300 GHz*, Instytut Medycyny Pracy im. prof. J. Nofera, Łodź 2009.

[5] http://wsse.krakow.pl/strona/index.php/obszary-dzialan/nadzor-sanitarny/108-promieniowanie/67-bezpieczne-korzystanie-z-telefonow-komorkowych (available: 03.11. 2017).

[6] Kuciński S., *Wpływ telefonii komórkowej na zdrowie człowieka*, II Krajowa Konferencja Naukowo-Techniczna „Ekologia w Elektronice", Warszawa 5-6.12.2002.

[7] Christian P. Karger, *Mobile phones and health: A literature overview*, Z. Med. Phys., 2005, 15, pp. 73-85.

[8] Fazlul Hoquel A.K.M., Sazzad Hossain Md., Sattar Mollah A., Akramuzzaman Md., *A study on specific absorption rate (SAR) due to non-ionizing radiation from wireless/ /telecommunicationin Bangladesh*, American Journal of Physics and Applications, 2013, 1(3), pp. 104-110.

POMIAR NATĘŻENIA SKŁADOWEJ ELEKTRYCZNEJ POLA ELEKTROMAGNETYCZNEGO SYGNAŁU FAL RADIOWYCH EMITOWANYCH PRZEZ WYBRANE TELEFONY KOMÓRKOWE

Obecnie stale obserwuje się wzrost liczby użytkowników telefonów komórkowych na całym świecie. Powoduje to zainteresowanie zagadnieniem wpływu promieniowania elektromagnetycznego na organizm ludzki. Źródłem pola elektromagnetycznego jest m.in. telefonia komórkowa, która składa się z dwóch podstawowych elementów: telefonów (terminali) i stacji bazowych. Współczynnik absorpcji swoistej (SAR) oznacza jednostkę energii o częstotliwości radiowej zaabsorbowanej przez ludzkie ciało podczas korzystania z telefonu komórkowego. Celem pracy było zmierzenie natężenia pola elektrycznego sygnału fal radiowych emitowanych przez wybrane telefony komórkowe. Pomiary przeprowadzono w Laboratorium Pomiarów Promieniowania w Wojewódzkiej Stacji Sanitarno-Epidemiologicznej w Rzeszowie. Pomiary przeprowadzono dla urządzeń pracujących w różnych systemach transmisji danych, działających w określonych pasmach częstotliwości. Pomiary wykonano za pomocą wywzorcowanego, uniwersalnego, szerokopasmowego miernika natężenia pola elektromagnetycznego typu NBM-550 nr B-0240 z sondą pomiarową typu EF-1891. Wskazania urządzeń sprawdzano dla włączonej i wyłączonej transmisji danych podczas odebrania i w trakcie łączenia sygnału. Opisano telefonię komórkową i podstawowe cechy tej technologii. W ostatniej części artykułu przedstawiono sposób wykonania pomiarów i wyniki.

Słowa kluczowe: pole elektromagnetyczne, telefonia komórkowa, stacje bazowe, SAR

Recived: 13.11.2017
Accepted: 25.11.2017

Jan A. MAMCZUR[1]

A PROOF OF NON-EXISTENCE OF SELF-IMAGING PHENOMENON IN THE INCOHERENT CASE

The existing description of incoherent wave field propagation in terms of Fourier transformation has made possible to prove non-existence of the self-imaging phenomenon for incoherent images.

Keywords: optical data processing, image formation theory, optical transfer functions, optical morphological transformations, spatial filtering, Fourier optics, Fourier transforms

INTRODUCTION

Self-imaging is meant in this paper as the phenomenon that occurs during propagation of an image in homogeneous isotropic stationary dielectric medium and consists in reconstruction of the original wave field intensity distribution in the plane distance z away from the original image. The authors approach to the self-imaging problem in the analogous way as W.D. Montgomery did in coherent case [1], i.e. by using the propagation operator in the diagonal form. In incoherent case, the diagonalization by the Fourier transformation was presented in [2]. The essential results of [2] are collected in Section 2 of the present paper where monotonicity of the propagation operator has also been pointed out. These results has made possible to prove non-existence of self-imaging phenomenon for incoherent images, which is showed in Section 3.

1. THE DIAGONAL OPERATOR OF INCOHERENT WAVE FIELD PROPAGATION

As well as in the coherent case [1, 3], the propagation of an incoherent wave field can be described by the linear transformation of the wave field intensity distribution [4]:

[1] Corresponding author: Jan A. Mamczur, Rzeszow University of Technology, Powstancow Warszawy 8, 35-959 Rzeszow, Poland, phone: (17) 8651943, e-mail: janand@prz.edu.pl

$$I(x,y;z) = \hat{\boldsymbol{P}}_z I(x,y;0) = \int_{-\infty}^{+\infty}\int g(x-x',y-y';z)I(x',y';0)\,dx'dy' \qquad (1)$$

where $I(x,y;0)$ and $I(x,y;z)$ are wave field intensity distributions in the original plane and in the plane distance z away, respectively, and $\hat{\boldsymbol{P}}_z$ is the incoherent propagation operator [5]. The integral operator kernel $g(x,y;z)$ in Eq. (1) is a well-known function of x,y,z [2].

There exists a diagonal Fourier representation of the incoherent propagation operator, converting the Fourier transform $J(\omega_x,\omega_y;0)$ of wave field intensity distribution in starting plane to intensity transform $J(\omega_x,\omega_y;z)$ of wave field formed at the distance z [2]. This diagonal Fourier representation $G(\omega_x,\omega_y;z)$, defined by

$$J(\omega_x,\omega_y;z) = G(\omega_x,\omega_y;z)\,J(\omega_x,\omega_y;0) \qquad (2)$$

is the Fourier transform of the kernel $g(x,y;z)$. It was obtained by using [6]:

$$G(\rho;z) = F[g(x,y;z)] = \frac{\kappa k^2}{8\pi^2} z\rho K_1(z\rho) + \frac{\kappa}{32\pi^2}\rho^2 K_2(z\rho) \qquad (3)$$

where ω_x, ω_y are spatial angular frequencies having the sense of wave-vector projection on the axes x and y, K_1 and K_2 are the modified Bessel functions of second kind (MacDonald functions) of first and second order, respectively, κ is a positive real constant, k is the wave number, and ρ is the radius in spatial angular frequency domain defined by

$$\rho = \sqrt{\omega_x^{\,2} + \omega_y^{\,2}} \qquad (4)$$

Selection rule of the constant κ was showed in [2]. Equation (2) together with the transform $G(\rho;z)$ is a more convenient tool for calculations than Eq. (1) with kernel $g(x,y;z)$ thanks to the diagonalization of the incoherent propagation operator and to fast Fourier transformation efficiency.

When propagation distance z is fixed, the transform $G(\rho;z)$ is a decreasing function of angular frequency radius ρ. It can be proved by using the formula for modified Bessel function differentiation [7]:

$$K'_\nu(x) = -\tfrac{1}{2}\left(K_{\nu-1}(x) + K_{\nu+1}(x)\right) \qquad (5)$$

and the formula for replacing Bessel function of higher order with functions of lower orders [8]:

$$K_{\nu+1}(x) = K_{\nu-1}(x) + \frac{2\nu}{x} K_{\nu}(x) \tag{6}$$

which yields after substituting:

$$K'_{\nu}(x) = -K_{\nu-1}(x) - \frac{\nu}{x} K_{\nu}(x) \tag{7}$$

The function $G(\rho;z)$ derivative is equal:

$$\frac{\partial G(\rho;z)}{\partial \rho} = \frac{\kappa k^2}{8\pi^2} z K_1(z\rho) - \frac{\kappa k^2}{8\pi^2} z^2 \rho \left(K_0(z\rho) + \frac{1}{z\rho} K_1(z\rho) \right) +$$

$$+ \frac{\kappa}{16\pi^2} \rho K_2(z\rho) - \frac{\kappa}{32\pi^2} z\rho^2 \left(K_1(z\rho) + \frac{2}{z\rho} K_2(z\rho) \right) =$$

$$= -\frac{\kappa k^2}{8\pi^2} z^2 \rho K_0(z\rho) - \frac{\kappa}{32\pi^2} z\rho^2 K_1(z\rho) < 0 \tag{8}$$

There are the minus signs in front of both the derivative components, which together with the fact that modified Bessel functions are positive in real domain yields function $G(\rho;z)$ monotonicity.

2. THE PROBLEM OF SELF-IMAGING OF INCOHERENT WAVE FIELDS

If the self-imaging effect occurs in incoherent case than there is at least one wave field intensity distribution that maps to the identical distribution as a result of propagation at the distance z. Using the propagation Eq. (2) and allowing the two intensity distributions to differ by a multiplicative real constant, we can write this assumption as an eigenequation in the Fourier representation:

$$J(\omega_x, \omega_y; z) = G(\omega_x, \omega_y; z) J(\omega_x, \omega_y; 0) = C\, J(\omega_x, \omega_y; 0) \tag{9}$$

where C is a real constant. Like W.D. Montgomery [1] in coherent case, we can formulate a condition for the incoherent self-imaging wave field on the basis of the above equation: the Fourier transform $J(\omega_x,\omega_y;0)$ of intensity distribution of such wave field, being an eigenfunction of Eq. (9), must take on non-zero values only in the angular spatial frequency region $\{(\omega_x,\omega_y)\}$ that satisfy the condition:

$$G(\omega_x, \omega_y; z) \equiv G(\rho; z) = C \tag{10}$$

As it has been shown in Section 2, the function $G(\rho;z)$ is monotonic in the whole frequency domain. Therefore the eigenequation (9) may only have such nontrivial eigenfunctions $J(\omega_x,\omega_y;0)$ that take on non-zero values only at one spatial frequency radius ρ, i.e. in one circle-shaped spatial frequency region with a radius $\rho_o \neq 0$. The transform $J(\omega_x,\omega_y;0)$ is meant here to be trivial if it takes on non-zero value at $\rho = 0$ only, i.e. the corresponding intensity distribution $I(x,y;0)$ is uniform. On the other hand, intensity distribution of every image is non-negative and has positive average, and hence its Fourier transform is positive at the zero spatial frequency ρ. Because there is only one ρ_o, it yields $\rho_o = 0$, i.e. the wave field is trivial. Therefore there is a contradiction in the demand that a non-trivial transform of physical wave field intensity distribution is an eigenfunction of eigenequation (9). In other words, the self-imaging effect does not exist in incoherent case.

3. CONCLUSIONS

The diagonalized operator of incoherent propagation has made possible to prove non-existence of incoherent self-imaging phenomenon for non-trivial images. Only infinite incoherent image with uniform intensity distribution does not change as a result of propagation at a certain distance.

REFERENCES

[1] Montgomery W.D., *Algebraic formulation of diffraction applied to self-imaging*, J. Opt. Soc. Am., 1968, 58, p. 1112.

[2] Mamczur J.A., *Warunki numerycznej i optycznej realizacji rozwiązania odwrotnego problemu koherentnej propagacji obrazów* – praca doktorska, Wydział Matematyczno-Przyrodniczy Uniwersytetu Rzeszowskiego, Rzeszów 2003.

[3] Matczak M.J., Mamczur J.A., *Degenerate self-imaging Fourier filters*, Optoelectronics Review, 2001, 9(3), p. 336.

[4] Goodman J.W., *Introduction to Fourier Optics*, McGraw-Hill Book Company, New York 1968.

[5] Born M., Wolf E., *Principles of Optics*, Pergamon, New York 1980.

[6] Ditkin V.A., Prudnikov A.P., *Integral Transforms and Operational Calculus*, Pergamon Press, 1965.

[7] Nikiforov A.F., Uvarov V.B., *Special Functions of Mathematical Physics*, Birkhauser, Basel 1988.

[8] Bracewell R., *The Fourier Transform And Its Applications*, McGraw-Hill, New York 1999.

DOWÓD NIEISTNIENIA ZJAWISKA SAMOOBRAZOWANIA W PRZYPADKU NIEKOHERENTNYM

Na podstawie istniejącego opisu optycznej propagacji niekoherentnych pól falowych z zastosowaniem transformacji Fouriera udowodniono teoretycznie nieistnienie zjawiska samoobrazowania dla niekoherentnych obrazów.

Słowa kluczowe: przetwarzanie danych optycznych, teoria powstawania obrazów, transformaty optyczne, filtracja częstości przestrzennych, optyka fourierowska, transformaty Fouriera

Received: 30.11.2017
Accepted: 15.12.2017

Aleksander SOKOŁOWSKI[1]
Tomasz WIĘCEK[2]

A NEW ALGORITHM FOR TESTING THE PROPERTIES OF NONWOVEN FABRICS

The new algorithm to study the properties of nonwoven fabrics is presented in the paper. The algorithm consists in image processing of the image of the highlighted nonwoven fabric. From the image there are selected the bright areas, which means sparse distributions of the fibers. Because nonwoven fabrics are used, among others, as medical and filtration materials their structure has significant impact on their ownership. The software task is primarily determine the porosity of the material.

Keywords: algorithm, nonwoven fabrics, porosity

INTRODUCTION

Polymer-laid nonwoven fabric formation in melt-blowing process [1] creates huge technological problems. The structure of fabric, its properties and characteristics are influenced by such parameters as the moisture of the polymer, the temperature of formation at the separate zones of installation, the output and temperature of the air blowing out the melt, the take-up velocity of the nonwoven, the distance of the condenser from the spinning nozzle, and the thickness of the fibers received [2]. The quality of non-woven fabrics is very important due to the applications in many areas such as for example engineering, medicine. Nonwoven with incorporated in its structure Triclosan, encapsulated in biodegradable polylactide, was studied for influence on the microbiological effect [3]. Nonwoven fabrics have been studied as a means of anti-allergenic protection against saprophytes [4]. Chitin nonwoven fabrics have been applied as clinical wound dressing [5]. Nonwoven garment was tested as a means of reducing bacteria in the operation room [6]. Biomodification of nonwoven polyester fabrics have been used in serum free cultivation of tissue cells [7]. Nonwoven fabrics have been used to improve of the electrolyte in the Li-ion battery technology [8]. This kind of materials are

[1] Corresponding author: Aleksander Sokołowski, Rzeszow University of Technology, Powstancow Warszawy 8, 35-959 Rzeszow, Poland, phone: (17) 8651895, e-mail: alex5@prz.edu.pl
[2] Tomasz Więcek, Rzeszow University of Technology, e-mail: ftkwiece@prz.edu.pl

applicable in for example water filtration [9]. The influence of the technological parameters of the padding process was under investigation for the filtration properties of polyester nonwoven fabrics [10]. To study the properties of non-woven fabrics are also used numerical methods. Numerical simulations on nonwoven-fibrous were performed to determine material design space for energy storage device separators [11]. Finite element method analyses have been applied to simulate behavior of the nonwoven fabrics [12-14]. The system for detect fabric weave patterns with help of computer image processing and analysis has been developed [15]. A novel approach to assessing textile porosity by the application of the image analysis techniques has been presented in [16]. R.H. Gong and A. Newton [17] have been described image-processing technique for measuring the fiber orientation distribution in nonwoven fabrics. E. Ghassemieh, M. Acar, and H.K. Versteeg [18] developed the image analysis techniques for study microstructural changes in non-woven fabrics. B. Pourdeyhimi, R. Dent, and H. Davis [19] presented the development of of an image analysis technique using the Fourier transform of the image to evaluate orientation in a fibrous assembly. The aim of this paper is to designate the diaphanous areas in nonwoven fabrics and their selected statistical parameters by means of numerical methods.

1. NUMERICAL ALGORITHM

The analyzed image is showed on Fig. 1. It shows the highlighted image of polymer-laid nonwoven fabric. It can be seen the brighter areas to be analyzed. The study of such images must consist of several stages. The first one should rely on image processing. The algorithm provides as first to convert a color image to image with levels of gray.

There are many methods of such transformations. One of them is to present only one color component of the color image. Because the human eye is most sensitive to green color and the least on the blue color, so the method described by Eq. (1) has been chosen in this paper.

$$R_{gr} = G_{gr} = B_{gr} = 0.2126 \cdot R_{col} + 0.7152 \cdot G_{col} + 0.0722 \cdot B_{col} \tag{1}$$

where R_{gr}, G_{gr}, B_{gr} denotes the base colors, red, green, and blue of image with levels of gray, R_{col}, G_{colr}, B_{gr} denotes the basic colors of color image.

The converted image scaled in 256 levels of gray is presented on Fig. 2. Because the analysis of the bright area is needed, so it should be extracted from the image. It can be done by converting the image in gray levels into the image of two-color. It should be selected the limit below which the gray levels convert into black color, and above which the gray levels convert into white color. If this limit is chosen at the level of 200, then we get a picture with white spots of different sizes, as it is shown in Fig. 3.

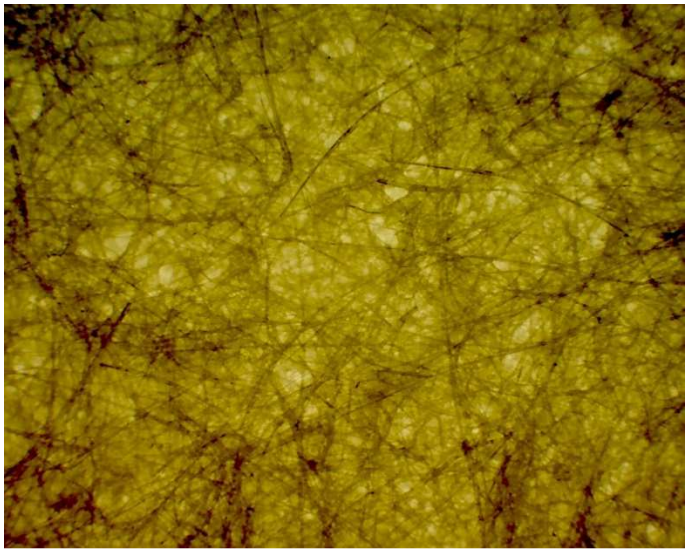

Fig. 1. The image of highlighted nonwoven fabric

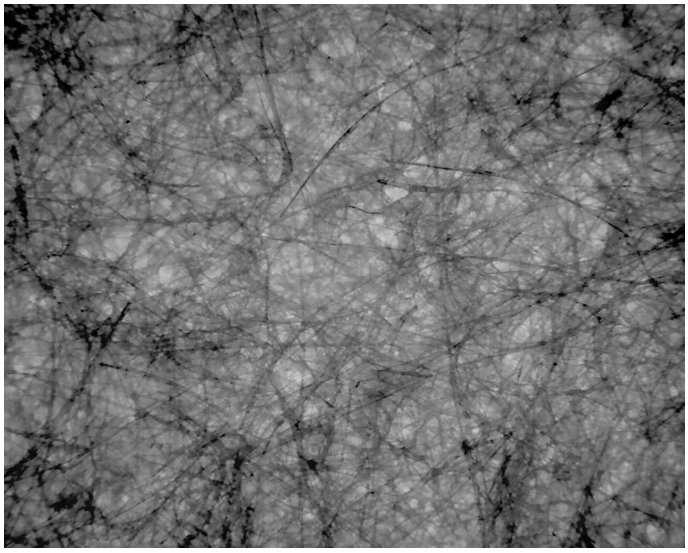

Fig. 2. Image from fig. 1 with color converted into the gray levels

The second part of algorithm is based on processing of white stains. The need is to locate any stain from a separate and process it. This is done by applying the so-called algorithm of mooving pixel. It is searching the first pixel lying on the edge of the stain. Then pixel goes around the edge of the stain and marks its inside. The number of pixels for each stain is counted at the same time. The process

is shown in Fig. 4, where an edge is marked with blue color and the inside with yellow color. If Figure 4 will be magnify, it can be seen the green pixels in the stains. They mean geometric centers of the stains.

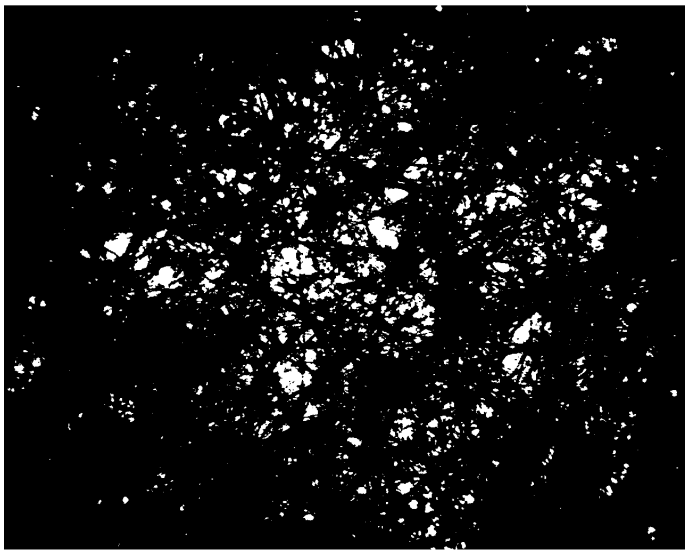

Fig. 3. Image from Fig. 2 converted into the image of black-white color

(a) (b)

Fig. 4. Image consists with several stains: a) before processing, b) after processing

The picture on Fig. 5 presents the image from Fig. 3 after processing. The software includes also the algorithms for calculating such quantities as the number of stains, the size of each stain, the coordinates of geometrical centers of the stains, etc.

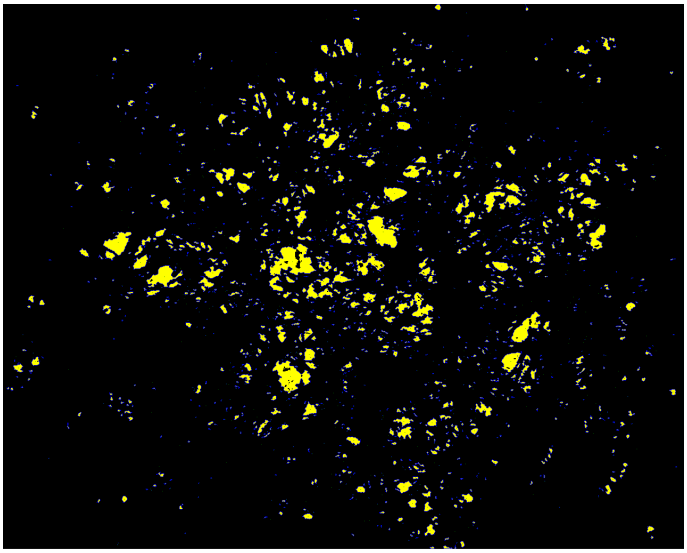

Fig. 5. Image from Fig. 3 after processing procedure

2. NUMERICAL RESULTS

This section shows selected numerical results obtained from the software based on the described algorithm. Table 1 presents selected parameters of the greatest 10 bright areas on the nonwoven fabrics from Fig. 1. The pixel coordinate 0, 0 lies in the upper left corner of the nonwoven fabric. Knowing the real size of nonwoven fabric, it is easy to find the position and the size of the stains.

Table 1. Selected results obtained for 10 greatest stains on the nonwoven fabric

The order down the size of the stains	**Pixel x – coordinate of the geometrical center**	**Pixel y – coordinate of the geometrical center**	**The size of the stain**
1	544	483	2932
2	541	700	2243
3	714	427	2136
4	303	514	1607
5	780	574	1527
6	983	611	1430
7	217	448	1301
8	689	489	952
9	995	672	923
10	1117	438	908

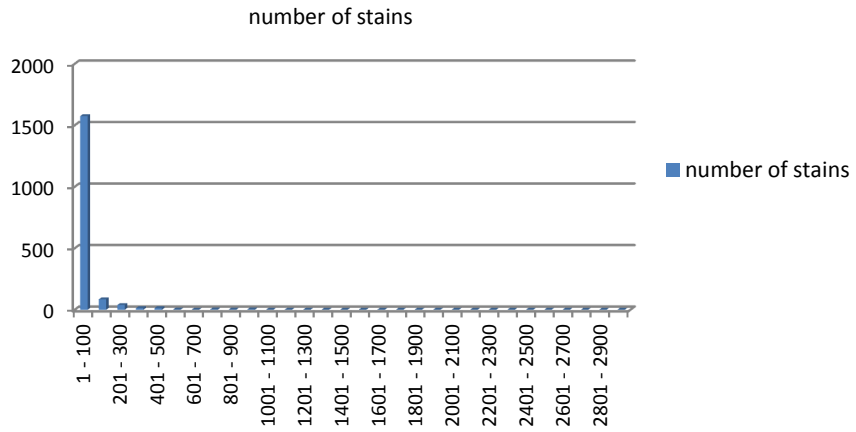

Fig. 6. Distribution of the stains according to their size

Figure 6 shows histogram of the distribution of the amount of stains, depending on their size. Because the number of all stains is 1743, and their size varies from 1 to 2932 pixels, there are selected on the horizontal axis the size ranges of these stains (in this case every 100 pixels). It can be seen from Fig. 6 that the most of the stains are the smallest, but there are also larger pieces.

3. CONCLUSIONS

The numerical algorithm for testing the degree of porosity of the nonwoven fabrics is presented in the paper. Because the nonwoven fabrics are used in many areas of technology and medicine, the algorithm is a good tool for testing the quality of these materials. The software extracts the unevenness of the distribution of the fibers in nonwoven fabrics and thus can be used to specify their spatial structure.

Acknowledgement

We would like to thanks Ms. Michalina Falkiewicz-Dulik of The Institute of Leather Industry, Kraków Branch for making the nonwoven fabric image availably for our research.

REFERENCES

[1] Keller J.P. et al., US Patent 3,755,527, 1973.

[2] Świątek J., Jarzębowski J., Cichoń J., *Investigation of Fibre Diameter Distribution in Non-Woven Textiles for Medical Applications in Melt-Blown Polyester Technology*, FIBRES & TEXTILES in Eastern Europe, 2008, 16, 3, pp. 14-16.

[3] Goetzendorf-Grabowska B., Królikowska H., Bąk P., Gadzinowski M., Brycki B., Szwajca A., *Triclosan Encapsulated in Poli(L,L-lactide) as a Carrier of Antibacterial Properties of Textiles*, FIBRES & TEXTILES in Eastern Europe, 2008, 16, 3, pp. 102--107.

[4] Buczyłko K., Chwała C., Niekraszewicz A., Ciechańska D., Wagner A., *Evaluation of the Effect of Anti-Mite Fabric on the Well-Being of Patients with a Mite Allergy*, FIBRES & TEXTILES in Eastern Europe, 2008, 16, 4, pp. 121-125.

[5] Ohshima Y., Nishino K., Yonekura Y., Kishimoto S., Wakabayashi S., *Clinical Application of Chitin Non-Woven Fabric as Wound Dressing*, European Journal of Plastic Surgery, 1987, 10, 2, pp. 66-69.

[6] Whyte W., Hodgson R., Bailey P.V., Graham J., *The reduction of bacteria in the operation room through the use of non-woven clothing*, British Journal of Surgery, 1978, 65, 7, pp. 469-474.

[7] Gümüşderelioğlu M., Türkoğlu H, *Biomodification of non-woven polyester fabrics by insulin and RGD for use in serum-free cultivation of tissue cells*, Biomaterials, 2002, 23, 19, pp. 3927-3935.

[8] Song M.K., Kim Y.T., Cho J.Y., Cho B.W., Popov B.N., Rhee H.W., *Composite polymer electrolytes reinforced by non-woven fabrics*, Journal of Power Sources, 2004, 125, pp. 10-16.

[9] Sakpal P.P., Landage S.M., Wasif A.I., *Application of nonwovens for water filtration*, International Journal of Advanced Research in Management and Social Sciences, 2013, 2, 2, pp. 28-47.

[10] Grzybowska-Pietras J., Malkiewicz J., *Influence of Technologic Parameters on Filtration Characteristics of Nonwoven Fabrics Obtained by Padding*, FIBRES & TEXTILES in Eastern Europe, 2007, 15, 5-6, pp. 82-85.

[11] Tuncer E., l'Abee R., *Numerical modeling of non-woven fiber mats: Their effective mechanical and electrical properties, arXiv:1304.5513* [cond-mat.soft], (2013)

[12] Hou X., Acar M., Silberschmidt V.V., *Finite element simulation of low-density thermally bonded nonwoven materials: Effects of orientation distribution function and arrangement of bond points*, Computational Materials Science, 2011, 50, 2, pp. 1292--1298.

[13] Sabuncouglu B., Acar M., Silberschmidt V.V., *A parametric finite element analysis method for low-density thermally bonded nonwovens*, Computational Materials Science, 2012, 52, 1, pp. 164-170.

[14] Demirci E., Acar M., Pourdeyhimi B., Silberschmidt V.V., *Finite element modelling of thermally bonded bicomponent fibre nonwovens: Tensile behavior*, Computational Materials Science, 2011, 50, 4, pp. 1286-1291.

[15] Kang T.J., Kim C.H., Oh K.W., *Automatic Recognition of Fabric Weave Patterns by Digital Image Analysis*, Textile Research Journal, 1999, 69, 2, pp. 77-83.

[16] Çay A., Vassiliadis S., Rangoussi M., *On the use of image processing techniques for the estimation of the porosity of textile fabrics*, Waset Org., 2005, 2, pp. 72-76.

[17] Gong R.H., Newton A., *Image-analysis Techniques Part II: The Measurement of Fibre Orientation in Nonwoven Fabrics*, Journal of The Textile Institute, 1996, 87, 2, pp. 371-388.

[18] Ghassemieh E., Acar M., Versteeg H.K., *Microstructural analysis of non-woven fabrics using scanning electron microscopy and image processing. Part 1: development and verication of the methods*, Proc. Instn. Mech. Engrs Part L: J. Materials: Design and Applications, 2002, 216, pp. 199-207.

[19] Pourdeyhimi B., Dent R., Davis H., *Measuring Fiber Orientation in Nonwovens Part III: Fourier Transform*, Textile Research Journal, 1997, 67, 2, pp. 143-151.

NOWY ALGORYTM DO BADANIA WŁAŚCIWOŚCI WŁÓKNIN

Przedstawiono nowy algorytm do badania porowatości włóknin. Algorytm zawiera przetwarzanie obrazu podświetlanej włókniny. Na obrazie są zaznaczone jasne obszary, co oznacza rozrzedzoną dystrybucję włókien. Ponieważ włókniny są używane między innymi jako materiały medyczne i filtracyjne, ich struktura ma znaczący wpływ na ich właściwości fizyczne. Zadaniem oprogramowania jest przede wszystkim określenie porowatości materiału.

Słowa kluczowe: porowatość, włóknina, algorytm

Received: 16.11.2017
Accepted: 4.12.2017

Feliks STACHOWICZ[1]
Marta WÓJCIK[2]

ECOLOGICAL AND ECONOMICAL BENEFITS FROM SEWAGE SLUDGE HYGIENISATION WITH THE USE OF LIME IN A MEDIUM-SIZE TREATMENT PLANT

Sewage sludge classified as hazardous waste requires searching for advanced and more effective methods of utilization. Waste produced in treatment plants, should be subject to proper reprocessing on the grounds of health, economic and legal reasons. In treatment plants, hygienisation with the use of lime (CaO) is commonly applied. The main advantage of the aforementioned method is the growth of pH value of sewage sludge and the reduction of pathogens. Apart from this, sewage sludge hygienisation with the application of lime is characterized by the high costs associated with the acquisition of lime. Assuming the price of highly reactive lime ranging from EUR 67-82 per one tone, additional cost of approximately EUR 8600 is generated for a medium treatment plants per year. Additionally, the liming of sewage sludge requires the modernization of treatment plants and the acquisition of new equipment. But due to the fertilizing properties of aforementioned waste, the agricultural utilisation of sewage sludge is the best method for small and medium treatment plants. The financial feasibility analysis showed that the whole undertaking will pay off within 7 years. This paper presents the cost-effective analysis of sewage sludge hygienisation in medium municipal treatment plant. In this article, the main mechanism of process and the influence of liming on sewage sludge characteristics are also showed.

Keywords: sewage sludge, liming, sewage sludge hygienisation, sewage sludge management, cost analysis

INTRODUCTION

Sewage sludge has been defined as mineral and organic compound derived from treated wastewater. With the increasing number of new residents attached to the sewerage system and the tightening requirements concerning the wastewater quality all over the world, the production of aforementioned waste reached an alarming level [1]. Due to the specific chemical and physical properties of sewage

[1] Corresponding author: Feliks Stachowicz, Rzeszow University of Technology, Powstancow Warszawy 8, 35-959 Rzeszow, phone: (17) 8651538, e-mail: stafel@prz.edu.pl
[2] Marta Wójcik, Rzeszow University of Technology, e-mail: m.wojcik@prz.edu.pl

sludge, its treatment and utilization is a significant problem for wastewater treatment plants. In line with the restriction placed on landfill waste with a calorific value above 6 MJ/kg introduced on 1 January 2016, the most economically and environmentally-friendly method of sewage sludge utilization is its agricultural use [2]. The possibility of agricultural sewage sludge application is associated with the high content of nutrients and organic matter [3]. Additionally, the positive impact of sewage sludge on the plants growth was confirmed by different authors. Gondek and Filipek-Mazur [4] proved that sewage sludge has affected the increase of calcium in plants. From the economical point of view, the use of sewage sludge in agricultural practices or for reclamation is characterized by the lowest costs of approximately EUR 100 for 1 Mg sludge. In contrast, combustion and co-combustion of sewage sludge are more expensive, even fourfold (Table 1) [5, 6].

Table 1. Predicted costs of sewage sludge management using different methods

Ways of sewage sludge utilisation	**Average disposal costs for 1 Mg sewage sludge EUR**
Agricultural use	100
Composting	150
Combustion	350
Co-combustion	430

Agricultural and natural ways of utilization of sludge management are legally permitted if they do not exceed permissible concentrations of heavy metals and biogenic compounds, as stated in Regulation on Urban Sewage Sludge of 15 February 2015 [7].The agricultural value of municipal sewage sludge also depends on the content of pathogen microorganisms. Pathogens entering the soil could lead to both surface and ground water contamination [1]. Before the application of sewage sludge in agriculture, detailed research is required in order to not exceed the content of heavy metals and microorganism.

The reduction of pathogens might be reached with the use of hygienisation process. Yu et al. [8] divided hygienisation methods into two categories: Class A and Class B. In Class B, the amount of microorganism is reduced to below 2 million colony forming units (CFU) per gram of total solids dry weight. By contrast, Class A could lead to the microorganism reduction at less than 1000 most probable numbers (MPN) per gram of total solids dry weight. Podedworna and Umiejewska [9] also classified the hygienisation process as: thermal, chemical, biological and radiation disinfection (Fig. 1).

In Poland, sewage sludge hygienisation with the use of lime is commonly applied for disinfection purposes. The addition of lime into aforementioned waste results in the increase of pH value and the significant reduction of pathogens [10]. Additionally, the mixture of sewage sludge and lime might be used as a natural

and valuable fertilizer improving the plant growth. Detailed information concerning the hygienisation with the use of lime is included in further section of the article.

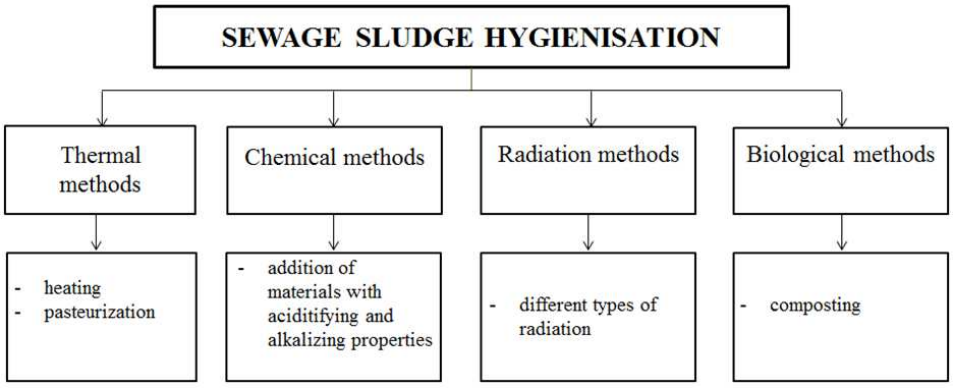

Fig. 1. Sewage sludge hygienisation methods

In Poland, there is a paucity of information on sewage sludge hygienization costs. Thus, this article presents the cost-effectiveness analysis of sewage sludge liming in a medium treatment plant. This paper also shows the impact of lime on sewage sludge properties and presents the main advantages associated with the application of aforementioned method in waste management.

1. THE MECHANISM OF SEWAGE SLUDGE HIGIENIZATION WITH THE USE OF LIME

Liming is commonly used as a conventional sewage sludge hygienisation method. According to different authors, the addition of lime into sludge contributes to the sludge stabilization and disinfection [7, 11]. The results of aforementioned processes are the immobilization of heavy metals and the change of structure of sewage sludge [7].

The main mechanism of sewage sludge hygienisation with the use of lime is based on the exothermic hydration reaction of calcium oxide, by the following equation (1) [11]:

$$CaO + H_2O \rightarrow Ca(OH)_2 + 1160\ kJ/kg\ CaO \quad (1)$$

For sewage sludge, the aforementioned reaction might be written as follows (2) [10]:

$$CaO + H_2O \rightarrow Ca(OH)_2 + 1160\,kJ/kg\,CaO\ + \text{stabilized sewage sludge} \quad (2)$$

As a result of the aforementioned reaction, hydroxyl ions are formed. It is estimated that 1 kg of CaO delivers 0,607 kg of OH^- ions. This phenomena results in the increase of alkalinity and the pH value of sewage sludge. Additionally, hydroxyl ions are highly toxic for pathogens and cause the change in ionization of microorganisms cells [11]. As a consequence, the activity of many enzymes could disappear. The results obtained by different authors [10, 12] confirmed that the high pH of sewage sludge is a major factor which influences the disappearance of compounds of proteins, especially in anion and carboxyl groups. For this reason, the growth of pH is a main destructive factor for pathogens in hygieniesation process. The research proved that most of bacteria and viruses contained in sewage sludge are inactivated in the pH above 9 [11]. In addition, ammoniac emitted during the hygienisation process, penetrates through cell membranes and intensifies the reduction of pathogens.

The literature review confirms that 1 kg of CaO absorbs approximately 0.32 kg of water and calcium hydroxide is formed [7, 11]. In line with the mass conservation law, the reaction might be written as follows (3) [10]:

$$1\text{kg}\,\text{CaO} + 0.324\ \text{kg}\ \text{H}_2\text{O} \rightarrow 1.324\ \text{kg}\ \text{Ca(OH)}_2 + 1160\ \text{kJ/kg}\,\text{CaO} \qquad (3)$$

Depending on the amount of emitted warmth, about 0.5 kg of water is evaporated. As a result, sewage sludge is dried and the growth of sludge dry mass is observed [11].

Secondly, hydrated lime contained in sewage sludge reacts with carbon dioxide from the atmosphere and carbonate calcium is created, by the following equation (4) [7, 11]:

$$\text{Ca(OH)}_2 + \text{CO}_2 \rightarrow \text{CaCO}_3 + \text{H}_2\text{O} + 1678\,\text{kJ/kg}\,\text{CaO} \qquad (4)$$

In line the mass conservation law, this reaction might be written as follows (5) [10]:

$$1,324\text{kg}\text{Ca(OH)}_2 + 0,776\text{kg}\text{CO}_2 \rightarrow 1,776\text{kg}\text{CaCO}_3 + 0,324\text{kg}\text{H}_2\text{O} +$$

$$+1678\,\text{kJ/kg}\,\text{CaO} \qquad (5)$$

The aforementioned reaction contributes to further sewage sludge stabilization and the improvement of shear strength. During this stage of the process, such obtained energy is used to heating and drying of sludge [7, 10, 11].

The effectiveness of sewage sludge hygienisation with the use of lime is determined by physical, chemical and microbiological properties of waste. The essential factor influencing the process effectiveness is also the contact time be-

tween sludge and lime. According to Malej [13], almost 100% reduction of pathogens might be achieved after one hour contact time. Marcinkowski [10] also proved that *Salmonella* bacteria had died off after one hour contact time with the pH value at least 11.6. That is the reason why the application of lime in sewage sludge treatment is justified.

2. METHODS

On the basis of investment and operation costs, financial feasibility analysis was calculated. The analysis included the calculation of the following elements: payback period (PP), net present value (NPV), profitability index (PI), internal rate of return (IRR), cash inflow (CIF), cash outflow (COF) and cash flow (CF).

Payback period (PP) was calculated as shown by the following equation:

$$PP = \frac{W}{Z}$$

where: PP – payback period, year; X – capital spending, EUR; Y – average annual investment income, EUR.

Net present value (NPV) was estimated by the following equation:

$$\mathrm{NPV} = \sum_{t=1}^{i} \frac{C_t}{(1+r)^t} - C_o$$

where: NPV – net present value, -; C_t – net cash inflow during the period t, EUR; C_o – total initial investment costs, EUR; r – discount rate, %; t – number of period times, -.

Profitability index (PI) was solved by the equation below:

$$\mathrm{PI} = \frac{\sum_{t=1}^{n} \frac{CF_t}{(1+r)^t}}{I}$$

where: PI – profitability index, -; C_o – net after-tax cash flow in year t, EUR; r – cost of capital, EUR; t – capital investment project's cash outlay assumed to occur in the current year, n – number of year, -.

Internal rate of return (IRR) was calculated by the following below:

$$\mathrm{IRR} = r_a + \frac{\mathrm{NPV}_a \cdot (r_b - r_a)}{(\mathrm{NPV}_a - \mathrm{NPV}_b)}$$

where: IRR – internal rate of return, -; r_a – lower discount rate chosen, %; r_b – higher discount rate chosen, %; NPV_a – NPV at rate *a*, -; NPV_b – NPV at rate *b*, -.

The influence of lime on the properties of sewage sludge was evaluated on the basis of pH value and the sewage sludge dry mass. pH of sewage sludge after hygienisation was analyzed with pH-meter HACH HQ40d according to PN-EN 15933:2013-02. In order to asses a dry mass, sewage sludge was dried at 105°C. The aforementioned parameter was calculated as shown by the following equation:

$$d.m. = \frac{m_s}{m_u} \cdot 100\%,$$

where: *d.m.* – sewage sludge dry mass, %; m_s – mass of sludge after drying, g; m_u – mass of hydrated sludge, g.

3. THE COST ANALYSIS OF SEWAGE SLUDGE HYGIENISATION BY MEANS OF LIME

The layout of devices for sewage sludge hygienisation is shown in Fig. 2. The complete technology of sewage sludge hygienisation consists of: the lime container, the lime feeder, the lime dispenser, the screw feeder of lime, the mixer of sludge and lime, the screw feeder of sludge and the screw feeder of obtained product. As wastewater treatment and previous stages of sludge treatment are not considered in the cost analysis, they are eliminated from this scheme.

Design criteria regarding the sewage sludge hygienisation in a medium treatment plant are shown in Table 2. This data and information were selected from manufacturer's index cards. Based on the calculation, the number of equipment was selected in order to fit proper conditions and requirements.

The cost analysis of sludge hygienisation was calculated and presented in Table 3. The value of equipment was obtained from EKO-MONTAŻ company. The presented analysis includes only the costs of necessary equipment and lime. The detailed cost analysis also requires determining the energy costs associated with the installation working.

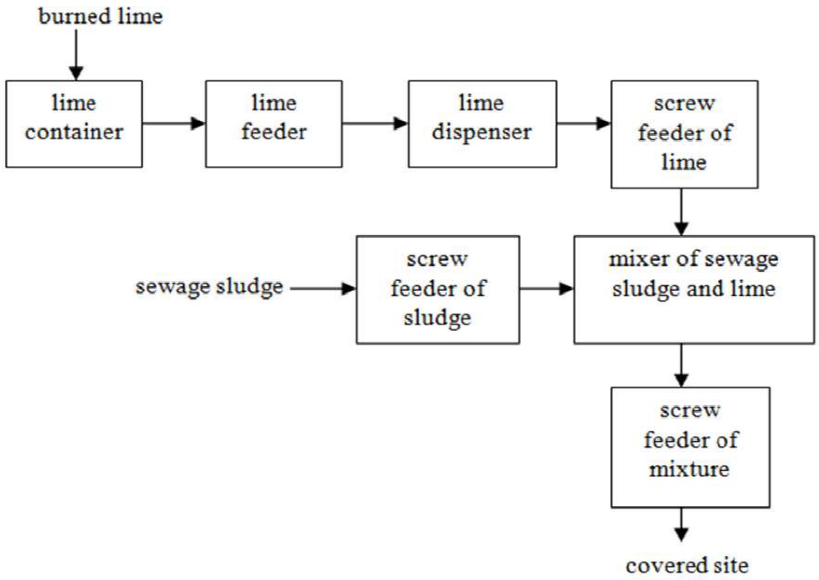

Fig. 2. Layout of devices for sewage sludge hygienisation in considered treatment plant

Table 2. Design parameters of equipment for sewage sludge hygienisation

Device	Design parameter	Number of devices
Lime container	volume: 20-30 m^3	1
Lime feeder	capacity: 1.5-2 m^3/h	1
Lime dispenser	capacity: 1.5-2 m^3/h	1
Screw feeder of lime	capacity: 1.5-2 m^3/h	1
Screw feeder of sewage sludge	capacity: 1.5-2 m^3/h	1
Mixer of lime and sewage sludge	capacity: 2 m^3/h	1
Screw feeder of obtained product	capacity: 1.5-2 m^3/h	1

The installation for lime dosing consists of the container with a volume in the range of 20-30 m^3, the lime feeder, the dispenser and the screw feeder which is responsible for the transport of lime. Additionally, the lime container is equipped with scrubbers. In order to avoid the lime agglomeration, special electrovibrators are located in the side wall of the container. In the bottom part of the device, there is a knife gate and the lime feeder. When the knife gate is opened, lime is given to the feeder containing the knife deflector. The rotation of the knife detector results in the transport of lime into the dispenser. The amount of lime is precisely controlled by the regulation of routes of screw feeder. The investment costs associated with the acquisition of aforementioned devices is approximately EUR 21 400. However, it will be also necessary to include additional costs associated with the energy consumption by the aforementioned devices (0.5-4.5 kWh) and workers training.

Table 3. Average costs of equipment and reagent for sewage sludge hygienisation

Device	Cost EUR
Lime container	16 000
Lime dispenser	2 500
Screw feeder of lime	2 900
Screw feeder of sewage sludge	4 400
Mixer of lime and sewage sludge	10 000
Screw feeder of obtained product	4 400
Automatic regulation	3 200
Transport of devices	14 000
Lime	8 600
COST	66 000

The transport of dewatered sewage sludge into the mixer is ensured by the screw feeder of sludge. For a medium treatment plant, the capacity of aforementioned device should be in the range of 1.5-2.0 m^3/h. The screw feeder consists of: the trough with chute, the charging hopper, the so-called screw and the power unit. The part of aforementioned elements is made from sheet steel. In the bottom part of a trough, there are special holes enabling the water evaporation. The transported material is given to the dispenser by means of a hole in a lid. The main advantage of screw feeders is the possibility to integrate with other devices, for example: filter press for sewage sludge dewatering. The costs associated with the acquisition of a screw feeder is approximately EUR 4 400. The operation costs are mainly associated with the energy consumption of about 4.5 kWh. During the exploitation of a screw feeder, it is necessary to avoid the full inflation of feeder in order to prevent friction between a trough and sewage sludge. The experimental tests proved that the full inflation of aforementioned device could contribute to the blockage of rotation of a screw.

The mixing of sewage sludge with lime is ensured by the application of a mixer. Depending on the kind and the moisture content of sludge, a twin-screw or paddle mixer is applied. The whole process is controlled by means of control cabinet. The mixer of sludge and lime is made from sheet steel and consists of two steel containers. One of them is filled with lime and the other is filled with dewatered sewage sludge. The sewage sludge hygienisation with the use of lime results in the increasing of temperature and the pH value which could contribute to the reduction of pathogens in waste. Such obtained mixture has a consistent structure and might be transported by means of the screw feeder to a covered site. The average cost of a mixer is approximately EUR 10 000. The price of a screw feeder is about EUR 4 400. However, it might be also necessary to include additional costs associated with the energy consumption.

In sewage sludge hygienisation, burned lime CaO is applied. The dosage of aforementioned reagent depends on the sewage sludge moisture content, the concentration of chemical compounds and the microbiological characteristics of waste. The literature review showed that the dosage of lime in sewage sludge liming is in the range of 0.15-0.25 kg CaO/kg d.m. In practice, the amount of applied burned lime is in the range of 22-23% of sewage sludge dry mass. In order to obtain the high effectiveness of sludge hygienisation, lime with a high level reactive is typically used. It is recommended to apply burned lime with a value of TS_{60} parameter below 1 minute. Depending on the distance of transport, the cost of 1 Mg of burned lime is in the range of EUR 67-82.

The above-mentioned cost analysis showed that the total costs of installation for sewage sludge hygienisation with the use of lime is approximately EUR 66,000. But the presented cost analysis includes only the price of devices and the applied reagent. One should also take into consideration additional costs associated with the workers training and the assembly of aforementioned devices.

Table 4. Financial feasibility analysis of sewage sludge hygienisation

Parameter	**Unit**	**Value**	**Profitability of investment**
PP (Payback period)	year	7	-
NPV (Net present value)	-	2241.61	>0
PI (Profitability index)	-	1.034	>1
IRR (Internal rate of return)	%	0.00	-
CIF (Cash inflow)	EUR	200 000	-
COF (Cash outflow)	EUR	186 000	-
CF (Cash flow)	EUR	14 000	-

The financial feasibility analysis was presented in Table 4 and in Fig. 3. The profit of treatment plant was calculated by the comparison of sewage sludge hygienisation and agricultural utilization with the landfilling and combustion of waste. The operation costs included the price of lime and other media required in the aforementioned process. By taking the annual profit from the sewage sludge hygienisation in a treatment plant of approximately EUR 10 000 and the annual operating cost of about EUR 20 000, the investment will pay off within 7 years. Additionally, other financial parameters confirm the profitability of sludge hygienisation. It is worth highlighting that the product of sewage sludge hygienisation might be further managed as a fertilizer in agricultural practices. By means of that, it is possible to eliminate the storage of sewage sludge gradually.

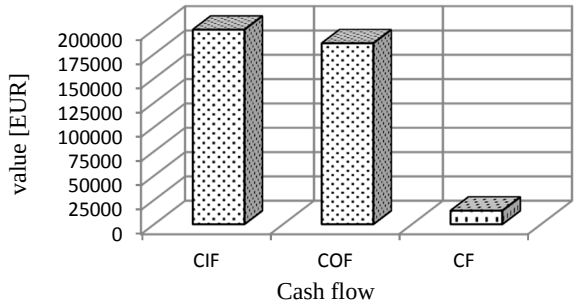

Fig. 3. Chart of cash flow

4. THE INFLUENCE OF LIME ON SEWAGE SLUDGE CHARACTERISTICS

Apart from the high temperature, the main factor that affects the reduction of microorganisms is the high pH value of sewage sludge after hygienisation. It is commonly known that the high concentration of hydroxyl ions resulted in the change of protein's ionization. As a consequence, the activity of many pathogens has decreased [11].

The influence of lime on pH of sewage sludge after hygienisation was presented in Fig. 4. After the application of burned lime in the amount of 10% of sewage sludge dry mass, the pH value increased by 106%. The aforementioned results were consistent with findings made by Marcinkowski [14] and Bazeli [12]. However, the pH value of sewage sludge was decreasing all the time. After 24 hours contact time of sewage sludge and lime, the pH decreased by approximately 5% to the value of 12.85 (Fig. 5). Consequently, the long-time storage of sewage sludge after hygienisation results in the decrease of pH and could contribute to the secondary growth of pathogens [15].

The influence of lime on sewage sludge dry mass was shown in Fig. 6. The obtained results confirmed the positive impact of aforementioned reagent on the decreasing moisture content. After the application of burned lime in the amount of 10% of sewage sludge dry mass, the pH value increased by approximately 16%. Similar results were achieved by other authors [12, 14]. This phenomena is caused by the heat emission, which results in the evaporation of water from sewage sludge. The influence of lime on the sewage sludge moisture content reduction contributes to the decreasing transport costs to places where sewage sludge will be utilized.

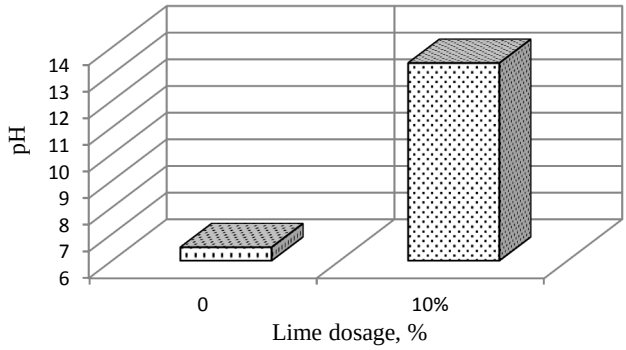

Fig. 4. The influence of lime on the pH value of sewage sludge

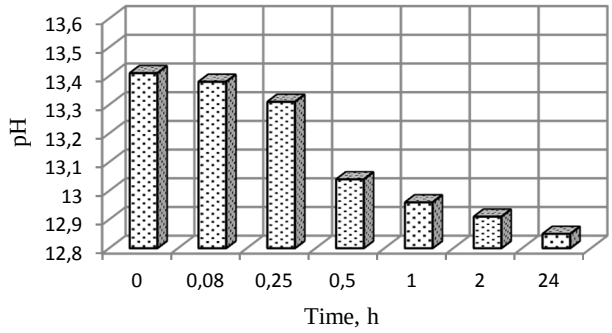

Fig. 5. The changes of pH value over time

Another advantage of hygienisation is the fact that obtained product might be successfully used in the cultivation of energy plants plantations. The aforementioned method allows retaining the turnover of nutrients, which closes the circuit elements in the local ecosystem [16, 17]. Moreover, chemical compounds contained in sewage sludge are excluded from the human food chain. Particular features of the energy plants construction help to take nutrients contained in sewage sludge without environmental contamination. For this reason, sewage sludge after hygienisation might be treated as an alternative for traditional mineral fertilizers, which in turn might successfully provide valuable nutrients for plants and could substitute popular fertilizers [6]. Additionally, energy plants have a high demand for nutrients and are characterized by a large absorbent surface [18]. The application of sewage sludge in energy plants plantations could help to achieve 20% share of renewable energy in final energy production in compliance with the requirements of the EU climate and energy package (3 x 20%).

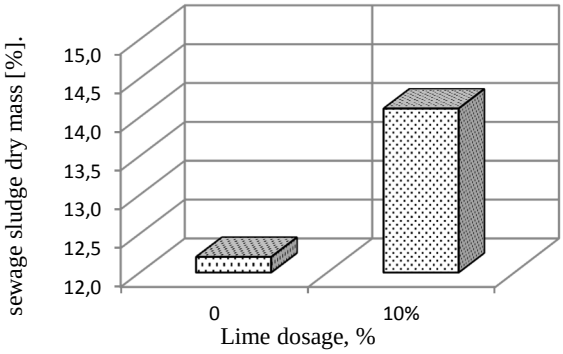

Fig. 6. The influence of lime on sewage sludge dry mass

5. CONCLUSIONS

The technology of sewage sludge hygienisation demonstrated the increase of pH and sewage sludge dry mass. However, the aforementioned process demands the acquisition of new devices for mixing and dosing of products, which increases the investment costs in treatment plant. The financial feasibility analysis showed that the whole undertaking will pay off within 7 years. Additionally, the mixture of sewage sludge and lime might be applied in agricultural practices, for example: in energy plants plantations. This investment could contribute to the elimination of sewage sludge storage in treatment plants.

Based on the results of cost-effectiveness analysis of investment, the following findings and conclusions could be made:

- the investment costs associated with the acquisition of equipment for sewage sludge hygienisation in a medium treatment plant is approximately EUR 66 000;
- prior to the implementation of aforementioned technology in treatment plants, it is necessary to choose the efficiency of the device. The proper selection of devices ensures the optimization of working conditions in a treatment plant;
- the annual costs of lime necessary in sewage sludge hygienisation is approximately EUR 8 600. In order to obtain the best process effectiveness, a high level reactive burned lime with a value of TS_{60} parameter below 1 minute is recommended;
- the financial feasibility analysis of the whole investment has shown that the technology of sewage sludge hygienisation is profitable and beneficial from the economical, environmental, legal and social point of view. It is estimated that the aforementioned investment will pay off within 7 years;
- the addition of lime to sewage sludge influences the growth of pH of sewage sludge. The addition of 10% of lime to sewage sludge results in

the increase of pH of approximately 106% to the value of 13.41. The high pH value of sewage sludge after hygienisation could contribute to the reduction of pathogens in a significant way. As the decline of pH is possible in time, the control of sanitary and microbiological characteristics of sewage sludge is necessary;

- additionally, the application of burned lime to sewage sludge results in the increase of dry mass. The sewage sludge moisture reduction could decrease the cost of transport to the places of its utilization;
- what is more, the mixture of lime and sewage sludge might be successfully used in the cultivation of energy plants plantations. The aforementioned method allows retaining the turnover of nutrients, which closes the circuit elements in the local ecosystem. The aforementioned application of sewage sludge after hygienisation could help to achieve 20% share of renewable energy in final energy production in compliance with the requirements of the EU climate and energy package (3 x 20%).

REFERENCES

[1] Zahin M.W., *Cost analysis of trickling-filtration and activated-sludge plants for the treatment of municipal wastewater*, Proceeding of the Seventh Saudi Engineering Conference, 2nd-5th December 2014, Ritadh, Saudi Arabia, 2, pp. 67-81.

[2] Regulation of the Minister of Economy of July 16, 2015 on the Acceptance of Waste for Landfill [J. of Laws from 2015, item 1277].

[3] Niemiec W., Wójcik M., *Możliwości wykorzystania komunalnych osadów ściekowych w wybranych oczyszczalniach*, ZN Mechanika, 2015, 87, 4, pp. 339-347.

[4] Gondek K., Filipek-Mazur B., *Akumulacja mikroelementów w biomasie owsa oraz ich dostępność w glebie nawożonej kompostem z odpadów roślinnych*, Acta Agrophysica, 2006, 8, 3, pp. 579-590.

[5] Henclik A., Kulczycka J., Gorazda K., Wzorek Z., *Uwarunkowania gospodarki osadami ściekowymi w Polsce i Niemczech*, Inżynieria i Ochrona Środowiska, 2014, 17, 2, pp. 185-197.

[6] Niemiec W., Stachowicz F., Trzepieciński T., Wójcik M., *Land-Applying Municipal Sludge in Energetic Willow Plantations*, Proceedings of The International Multidisciplinary Conference, 12th Edition, 24th-26th May 2017, Baia Mare – Nyireghaza, pp. 69-72.

[7] Regulation of Minister of Environment of 6 February 2015 on Urban Sewage Sludge [J. of Laws from 2015, item 257].

[8] Yu Y., Chan W.I., Liao P.H., Lo K.V., *Disinfection and solubilization of sewage sludge using the microwave enhanced advanced oxidation process*, Journal of Hazardous Materials, 2010, 181, pp. 1143-1147.

[9] Podedworna J., Umiejewska K., *Technologia osadów ściekowych*, Oficyna Wydawnicza Politechniki Warszawskiej, Warszawa 2008.

[10] Marcinkowski T., *Przetwarzanie osadów ściekowych w procesie wapnowania*, Polskie Zrzeszenie Inżynierów i Techników Sanitarnych, Poznań 2010.

[11] Bień J., Wystalska K., *Osady ściekowe – teoria i praktyka*, Seidel-Przywecki Publishing House, Częstochowa 2011.

[12] Bazeli M., *Higienizacja osadów ściekowych – wapnowanie*, Forum Eksploatatora, 2006, 24, 3, pp. 17-20.

[13] Malej J., *Właściwości osadów ściekowych oraz wybrane sposoby ich unieszkodliwiania i utylizacji*, Rocznik Ochrona Środowiska, 2000, 2, pp. 69-101.

[14] Marcinkowski T., *Stosowanie różnych form wapna w procesach przetwarzania komunalnych osadów ściekowych. Część 3. Przetwarzanie osadów tlenkiem wapnia*, Forum Eksploatatora, 2009, 41, 2, pp. 39-41.

[15] Marcinkowski T., *Decontamination of Sewage Sludges with Quicklime*, Waste Management & Research, 1985, 3, pp. 55-64.

[16] Stachowicz F., Trzepieciński T., Wójcik M., Masłoń A., Niemiec W., Piech W., *Agricultural utilisation of municipal sludge in willow plantation*, E3S Web of Conferences, 2016, 10, pp. 1-6.

[17] Niemiec W., Stachowicz F., Trzepieciński T., Wójcik M., *Obróbka komunalnego osadu ściekowego przeznaczonego do nawożenia plantacji roślin energetycznych*, [in:] *Zrównoważona gospodarka zasobami przyrodniczymi i kulturowymi na Pogórzu Dynowskim determinantą rozwoju turystyki*, Związek Gmin Turystycznych Pogórza Dynowskiego, Dynów 2017, p. 133-150.

[18] Rosikoń K., *Osady ściekowe w nawożeniu wybranych roślin energetycznych*, Inżynieria i Ochrona Środowiska, 2014, 17, pp. 339-348.

EKONOMICZNO-EKOLOGICZNE ASPETY TECHNOLOGII WAPNOWANIA OSADÓW ŚCIEKOWYCH NA PRZYKŁADZIE ŚREDNIEJ OCZYSZCZALNI ŚCIEKÓW

Wzrost świadomości społecznej dotyczącej zagrożenia spowodowanego niewłaściwie prowadzoną gospodarką odpadami skutkuje rozwojem nowych metod ich utylizacji, zgodnie z wymogami prawnymi ekologicznymi i społecznymi. Celem implementowania nowych zasad gospodarki odpadami wprowadzane są nowe lub zaostrzane dotychczas obowiązujące akty prawne, mające kształtować prawidłowe strategie postępowania z odpadami. Intensyfikacja zabudowy i przyłączanie do systemu zbiorowego odprowadzania ścieków nowych odbiorców skutkuje produkcją ogromnych ilości osadów ściekowych. Specyficzne właściwości ubocznych produktów oczyszczania ścieków wymagają poszukiwania nowych metod ich przeróbki i unieszkodliwiania zgodnie z zasadami ochrony środowiska, z jednoczesnym uwzględnieniem aspektów ekonomicznych. Ze względu na obecność mikroorganizmów patogennych w osadach ściekowych, proces higienizacji osadów ściekowych jest jednym z najważniejszych etapów ich przeróbki. Studium literatury potwierdza, że powszechnie w oczyszczalniach ścieków stosuje się proces wapnowania z użyciem CaO. Niewątpliwą zaletą wspomnianego procesu jest możliwość redukcji patogenów do bezpiecznego poziomu, umożliwiającego dalsze zagospodarowanie osadów ściekowych w zabiegach przyrodniczych. Aplikacja wapna palonego w procesie higienizacji osadów ściekowych generuje jednak wysokie koszty eksploatacyjne oczyszczalni ścieków, związane z zakupem wspomnianego reagenta. Przy średniej cenie wysokoreaktywnego wapna na poziomie 67-82 euro za tonę, roczne koszty zakupu reagenta niezbędnego do procesu higienizacji wynoszą około 8 600 euro w przypadku średniej oczyszczalni ścieków. Dodatkowo, wdrożenie technologii wapnowania osadów ściekowych wiąże się z koniecznością modernizacji istniejącego ciągu technologicznego części osadowej i zakupem nowych urządzeń. Analiza opłacalności inwestycji wykazała jednak, że wprowadzenie procesu higienizacji

w średniej oczyszczalni ścieków może się zwrócić po około 7 latach. Prezentowany artykuł przedstawia analizę ekonomiczną wdrożenia procesu wapnowania osadów ściekowych na przykładzie średniej oczyszczalni ścieków, z jednoczesnym wskazaniem korzyści ekologicznych.

Słowa kluczowe: osady ściekowe, wapnowanie, higienizacja, gospodarka osadami ściekowymi, analiza ekonomiczna

Received: 4.09.2017
Accepted: 10.10.2017

ADDITIONAL INFORMATION

The Journal annually publishes a list of reviewers: in the last issue of the quarterly - no. 4/2017 and on the website:
https://oficyna.prz.edu.pl/zeszyty-naukowe/physics-for-economy

The Journal uses as described on its website the procedure for reviewing:
https://oficyna.prz.edu.pl/zeszyty-naukowe/physics-for-economy/zasady-recenzowania/

Information for authors available at:
https://oficyna.prz.edu.pl/zeszyty-naukowe/physics-for-economy/informacje-dla-autorow/

Review's form available at:
https://oficyna.prz.edu.pl/zeszyty-naukowe/physics-for-economy/formularz-recenzji/

Instruction for Authors
https://oficyna.prz.edu.pl/zeszyty-naukowe/instrukcja-dla-autorow/

Contact details to Editorial Office available at:
https://oficyna.prz.edu.pl/zeszyty-naukowe/physics-for-economy

Electronic version of the published articles available at:
https://oficyna.prz.edu.pl/zeszyty-naukowe/physics-for-economy

Reviewing standards, information for authors, the review form, instruction for authors and contact details to „Physics for Economy" Editors and to Publishing House are also published in the fourth number of „Physics for Economy" (4/2017).

Circulation 40 + 22 copies. Publisher's sheet 3,17. Printer's sheet 4,0. Offset paper 80g B1.
Manuscript completed in December 2017, Printed in December 2017.
Printing Publishing House, Powstancow Warszawy 12, 35-959 Rzeszow
Order no. 156/17